572754

NASA/TM—2002-211477

Robust Parameter Design Methodologies for Optimal Micro-Scale Secondary Flow Control in Compact Inlet Diffusers

Bernhard H. Anderson
Glenn Research Center, Cleveland, Ohio

Dennis J. Keller
RealWorld Quality Systems, Cleveland, Ohio

March 2002

The NASA STI Program Office . . . in Profile

Since its founding, NASA has been dedicated to the advancement of aeronautics and space science. The NASA Scientific and Technical Information (STI) Program Office plays a key part in helping NASA maintain this important role.

The NASA STI Program Office is operated by Langley Research Center, the Lead Center for NASA's scientific and technical information. The NASA STI Program Office provides access to the NASA STI Database, the largest collection of aeronautical and space science STI in the world. The Program Office is also NASA's institutional mechanism for disseminating the results of its research and development activities. These results are published by NASA in the NASA STI Report Series, which includes the following report types:

- TECHNICAL PUBLICATION. Reports of completed research or a major significant phase of research that present the results of NASA programs and include extensive data or theoretical analysis. Includes compilations of significant scientific and technical data and information deemed to be of continuing reference value. NASA's counterpart of peer-reviewed formal professional papers but has less stringent limitations on manuscript length and extent of graphic presentations.

- TECHNICAL MEMORANDUM. Scientific and technical findings that are preliminary or of specialized interest, e.g., quick release reports, working papers, and bibliographies that contain minimal annotation. Does not contain extensive analysis.

- CONTRACTOR REPORT. Scientific and technical findings by NASA-sponsored contractors and grantees.

- CONFERENCE PUBLICATION. Collected papers from scientific and technical conferences, symposia, seminars, or other meetings sponsored or cosponsored by NASA.

- SPECIAL PUBLICATION. Scientific, technical, or historical information from NASA programs, projects, and missions, often concerned with subjects having substantial public interest.

- TECHNICAL TRANSLATION. English-language translations of foreign scientific and technical material pertinent to NASA's mission.

Specialized services that complement the STI Program Office's diverse offerings include creating custom thesauri, building customized data bases, organizing and publishing research results . . . even providing videos.

For more information about the NASA STI Program Office, see the following:

- Access the NASA STI Program Home Page at ***http://www.sti.nasa.gov***

- E-mail your question via the Internet to help@sti.nasa.gov

- Fax your question to the NASA Access Help Desk at 301–621–0134

- Telephone the NASA Access Help Desk at 301–621–0390

- Write to:
  NASA Access Help Desk
  NASA Center for AeroSpace Information
  7121 Standard Drive
  Hanover, MD 21076

NASA/TM—2002-211477

Robust Parameter Design Methodologies for Optimal Micro-Scale Secondary Flow Control in Compact Inlet Diffusers

Bernhard H. Anderson
Glenn Research Center, Cleveland, Ohio

Dennis J. Keller
RealWorld Quality Systems, Cleveland, Ohio

National Aeronautics and
Space Administration

Glenn Research Center

March 2002

Available from

NASA Center for Aerospace Information
7121 Standard Drive
Hanover, MD 21076

National Technical Information Service
5285 Port Royal Road
Springfield, VA 22100

Available electronically at http://gltrs.grc.nasa.gov/GLTRS

ROBUST PARAMETER DESIGN METHODOLOGIES FOR OPTIMAL MICRO-SCALE SECONDARY FLOW CONTROL IN COMPACT INLET DIFFUSERS

Bernhard H. Anderson
National Aeronautics and Space Administration
Glenn Research Center
Cleveland, Ohio 44135

Dennis J. Keller
RealWorld Quality Systems
Cleveland, Ohio 44116

ABSTRACT

It is the purpose of this report to study and evaluate three optimal Robust design methodologies for application towards micro-scale secondary flow control (MSFC) for the management of inlet recovery, engine face distortion and High Cycle Fatigue (HCF) in compact inlet diffuser. Robustness in this situation means that it is possible to design fixed MSFC Robust installation (i.e. open loop) which operates well over the range of mission variables and is only marginally different from adaptive (i.e. closed loop) installation design, which would require a control system. The three Robust methodologies include (1) the traditional Taguchi *Robust Parameter Design* methodology, (2) a "Higher Order" Robust method, which used the same DOE structure as Taguchi, but with an alternate analysis, and (3) a "Lower Order" economical approach to Robust Design, where a single DOE was established which was composed of both the inner array (design) variables and outer array (mission) variables. For each of the three Robust design methodologies, two different mission strategies were considered for the subject inlet, namely (1) Maximum Performance, and (2) Maximum HCF Life Expectancy. The Maximum Performance mission maximized total pressure recovery while the Maximum HCF Life Expectancy mission minimized the mean of the first five Fourier harmonic 1/2 amplitudes, i.e. "collectively" reduced all the Fourier harmonic 1/2 amplitudes of engine face distortion. Each of the mission strategies was subject to a low engine face distortion constraint, i.e. DC60 $\leq$ 0.10, which is a level acceptable for commercial engines.

Each of the three Robust methodologies examined in this report, (i.e. the Taguchi methodology, the "Higher Order" methodology, and the "Lower Order" methodology) provided installation designs that satisfied the two mission requirements. The two mission requirements were Maximum Performance and the Maximum HCF Life Expectancy objectives. For each of the six optimal Robust installation designs (i.e. the three methodologies and two mission strategies), the DOE model predicted performances were successfully validated with CFD verification runs (i.e. no substantial differences were found between the DOE model predictions and CFD validation results). Also, statistical comparison among the Optimal Robust performance of the three Robust methodologies indicated no significant differences between the Taguchi and the "Higher Order" methodologies and only minor differences between the "Lower Order" and the "Higher Order" and the Taguchi methodologies. This was true for both mission strategies. The slight dif-

ferences in final Robust Optimal performance were negligible when compare the differences that would be discernible in a Wind Tunnel experiment. Hence, even though all three methodologies were capable of finding a robust optima that satisfied the mission requirements, the "Lower Order" method provides an economical alternative where the number of runs is drastically reduced.

INTRODUCTION

The current development strategy for combat air-vehicles is directed towards reduction in the Life-Cycle Cost (LCC) with little or no compromise to air-vehicle performance and survivability. This strategy has been extended to the aircraft component level, in particular, the engine inlet diffuser system. One method to reduce inlet system LCC is to reduce its structural weight and volume. Consequently, advanced combat inlet configurations are being made more compact (or shorter) to achieve weight and volume (and LCC) reduction. However, compact S-duct diffusers are characterized by high distortion and low pressure recovery, produced by extreme wall curvature and strong secondary flow gradients. These characteristics are further aggravated by maneuver conditions. Since survivability rather than aerodynamic performance often drives the inlet design, it is expected that the flow quality entering the turbine engine will present an additional challenging environment for both fan/compressor surge margin and aeromechanical vibration. Interest in High Cycle Fatigue (HCF) research by the US aerospace community has been spurred by discrepancies between the expected durability of engine components compared to that actually experienced in the field. Recognizing that inlet distortion is a forcing function for vibration in the fan components, methods for increasing HCF Life Expectancy can been combined with techniques for inlet recovery and engine face distortion management. Therefore, to enable acceptable performance levels in such advanced, compact inlet diffuser configurations, micro-scale secondary flow control (MSFC) methods are being developed to manage the recovery, distortion, and HCF aspects of distortion.[1]-[2]

One of the most difficult tasks in the design of MSFC installation for optimal inlet operation is arriving at the geometric placement, arrangement, number, size and orientation of the effector devices within the inlet duct to achieve optimal performance.These effector devices can be activated by either mechanical or fluidic means.This task is complicated not only by the large number of possible design variables available to the aerodynamicist, but also by the number of decisions parameters that are brought into the design process. By including the HCF effects into the inlet design process, the aerodynamicist has a total of seven individual response variables which measure various aspects of inlet performance. They include the inlet total pressure recovery, the inlet total pressure recovery distortion at the engine face and the first five Fourier harmonic 1/2 amplitudes of distortion. Each of these responses needs to be either maximized, minimized, constrained or unconstrained while searching for the optimal combination of primary design variable values that satisfy the mission requirements. The design task is further complicated by the existence of hard-to-control factors which effect inlet performance, i.e. the mission variables. The mission variables that cause the off-design penalty are, for example, inlet throat Mach number (engine corrected weight flow), angle-of-incidence and angle-of-yaw. While the aerodynamicist does not know how the pilot is ultimately going to fly the aircraft, it is known how the mission variables effect inlet performance under wind tunnel conditions. Traditionally, tolerance or robustness to the mission variables was accomplished only after the parameter design was completed, usually by accepting whatever off-design performance was delivered by the newly

designed inlet system. Numerical optimization procedures that have been successful with some aerodynamics problems give little assistance to designing robust inlets since they are point-design procedures, usually with only one decision parameter. However, there is a branch of statistical Design-of-Experiments (DOE) methodology which integrates both traditional Response Surface Methods and Robustness considerations into a single optimization procedure. It presents new potential for further reduction of *total quality cost* over the traditional design approach.

Taguchi[3] coined the term *Robust Parameter Design* to describe an approach to industrial problem solving whereby the product variation is reduced by choosing levels of the control factors (design parameters) that make the product insensitive to the changes in the noise factors that represent sources of variations. These noise factors in industrial design are often the environmental variables, such as temperature and humidity conditions, properties of the material, and product aging. In some applications, they measure how the consumer uses or handles the product. In the aerodynamic design of inlet systems, there is a analogous situation to the industrial design problem. As mentioned above, the design of inlet systems is usually accomplished at the cruise condition (the on-design condition) while variations from the cruise condition are considered as an off-design penalty. Because the mission variables cause variation from on-design performance, they can be identified with the noise factors or environmental variables in the analogous industrial design problem. Likewise, how the pilot flies the aircraft can be identified with how the consumer uses or handles the product. In the industrial problem, the researchers must be able to control the environmental variables in a laboratory environment, even though they cannot be controlled at the production level or in the field. Likewise, the aerodynamic researcher can indeed control the mission variables in the wind tunnel environment, however these variables cannot be controlled in flight (in the field). By making the analogy between the industrial design problem and the aerodynamic design problem, *Robust Parameter Design* methods developed for industrial problem solving can be adapted to the design of inlet systems, and in particular, design of micro-scale secondary flow control installations for such inlet systems.

Much has been written and said about the contribution of Genichi Taguchi to the vastly important area of *Product Quality Enhancement.* However, much controversy surrounds Taguchi's methodology among statisticicans. Many statisticians have pointed out the apparent flaws in the Taguchi approach. However, it suffices to say the importance of Taguchi's contributions lies in the idea that process or product sensitivity to its environment can be incorporated into the optimal statistical Design-of-Experiment and subsequent analysis of data. To the aerodynamicist, it represents a quantum leap in the area of aerodynamic design. For the first time, the mission variables can be directly introduced into the aerodynamic design processes. The inlet system can now be designed to operate with optimal performance over a range of specified mission variables. Rigorous application of Taguchi's *Robust Parameter Design* method may not be optimal in the design of micro-scale secondary flow installations for inlet systems because: (a) it loses information vital to the aerodynamicist and, (b) it is costly. However, Taguchi's *Robust Parameter Design* method can be used to arrive at an optimal installation design.

In this report, three Robust optimal design methodologies were studied and evaluated. These include (1) the traditional Taguchi *Robust Parameter Design* methodology, (2) a "Higher Order" Robust method, which used the same DOE structure as Taguchi, but with an alternate analysis which does not lose information by collapsing the outer array matrix information into a S/N parameter, and (3) a "Lower Order" economical approach to Robust Design, where a single DOE was established which was composed of both the inner array (design) variables and outer array (mission) variables. For each of the three Robust design methodologies, two different

mission strategies were considered for the subject inlet, namely (1) Maximum Performance, and (2) Maximum HCF Life Expectancy. The Maximum Performance mission maximized total pressure recovery while the Maximum HCF Life Expectancy mission minimized the mean of the first five Fourier harmonic 1/2 amplitudes, i.e. "collectively" reduced all the Fourier harmonic 1/2 amplitudes of engine face distortion. Each of the mission strategies was subject to a low engine face distortion constraint, i.e. DC60 $\leq$ 0.10, which is a level acceptable for commercial engines.

NOMENCLATURE

AIP	Aerodynamic Interface Plane
c	Effector Chord Length
CCF	Central Composite Face-Centered
CFD	Computational Fluid Dynamics
D	Engine Face Diameter
DC60	Circumferential Distortion Descriptor
DOE	Design of Experiments
h	Effector Blade Height
HCF	High Cycle Fatigue
Fi/2	i^{th} Fourier Harmonic 1/2 Amplitude
FM/2	Mean Fourier Harmonic 1/2 Amplitude
L	Inlet Diffuser Length
LCC	Life Cycle Costs
MSFC	Micro-Scale Secondary Flow Control
Mt	Inlet Throat Mach Number
n	Number of Effector Vanes per Band
PFAVE	Inlet Total Pressure Recovery
RSM	Response Surface Methodology
R	Inlet Throat Radius
Re	Reynold Number per ft.
Xi	Generalized Factor Variable
Yi	Generalized Response Variable
α	Inlet Angle-of-Incidence
β	Effector Vane Angle-of-Incidence
γ	Inlet Angle-of-Yaw

RESULTS AND DISCUSSION

Design of the Experiment

The basic problem of experimental (CFD) design is deciding what pattern of test cases will best reveal aspects of the situation of interest. For that reason, the overall objectives of the study become very important. In the present study, three objectives were considered important, namely: (1) to determine the design characteristic of multi-installation micro-scale secondary flow control configurations, (2) to establish the ability of MSFC to manage the aeromechanical effects of engine face distortion, and (3) to evaluate the effectiveness of this new methodology for "open loop" micro-scale secondary flow installations over an angle-of-incidence range in compar-

ison to fully adaptive "closed loop" designs. The first two objectives of this overall study on micro-scale flow control are covered by Anderson and Keller,[4] while the third objective is covered in detail this report and in Anderson and Keller.[5] A forth report in this series by Anderson and Keller[6] evaluates the impact of rake geometry, specifically the number of rake arms, on the measurement errors associated with estimating the first five Fourier harmonic 1/2 amplitudes of engine face distortion.

The basic inlet flowpath chosen for this study featured a compact (L/D =3.0), two turn, or S-duct inlet diffuser, Figure (1). This S-duct was defined by AGARD FDP Working Group 13 Test Case 3, Willmer, Brown and Goldsmith[7], and was dubbed the DERA/M2129 inlet. Traditionally, this type of compact inlet duct would be excluded from design consideration since it is characterized by severe wall curvature that induces strong secondary flows. These strong secondary flow can cause a flow separation called vortex lift-off. See Figure (1). This type of 3D flow separation results in severe total pressure losses and severe engine face distortion. Figure (2) presents the engine face total pressure recovery contours and secondary flow velocity vectors for the DERA/M2129 inlet S-duct at a throat Mach number of 0.70 and at 0^{o} angle-of-incidence. A vortex pair was dominant in the engine face flow field which was accompanied by very severe engine face total pressure distortion.

To manage the flow in the DERA/M2129 inlet S-duct, a three-band installation arrangement of micro-scale effectors was placed in the upstream section near the inlet throat. See Figures (3) and (4). These micro-scale effectors were simple vanes, the largest height being about the average height of the momentum layer at station (3), or about 2.0 mm. The purpose of these simple vanes was to create a set of co-rotating vortices that would quickly merge to form a thin layer of secondary flow that would counter the formation of the passage vortex pair. Since the height of the vane effectors were limited to 2.0 mm, a multi-band arrangement was chosen to investigate the possibility of enhancing the effect of the individual vanes by adding more bands of effectors. The spacing between the bands was critical since interaction would occur between respective bands of effector units. The first band was placed at the inlet throat station, X/R = 0.0, while the second and third bands of effector vanes were placed nominally at X/R = 1.0 and at X/R = 2.0 respectively. See Figure (3). Nominally, the spacing between the effector vanes was DX/c = 4.0, i.e. about four effector chord lengths as measured between the half chord stations. See Figure (4).

The DOE approach followed directly from the three objectives previously stated and was reflected in the layout of the design factors listed in Table (1). The design variables (factors) were the effector vane heights (mm) in the three upstream installation h1, h2, and h3, and the inlet angle-of-incidence α. The effector vane heights were changed independently and, therefore, constituted three independent variables. Strictly speaking, the inlet angle-of-incidence was a mission variable and was, therefore, one of the noise factors that belonged with the environmental variables, i.e. the outer array in the traditional Taguchi-style DOE design. In the "Lower Order" approach, however, the angle-of-incidence was introduced into the statistical design matrix with the control factors. This allowed greater economy than the traditional Taguchi approach. Table (2) shows the variables that were held constant during this study. The number of micro-scale vane effectors, $n_{i,\ i=1,3}$, was held fixed at 24 in the half-plane, and were spaced symmetrically around the half-plane periphery. Each vane effector was set at a geometric vane angle-of-incidence $\beta_{i,\ i=1,3}$ of 24.0^{o}. In addition, the throat Mach Number (Mt), Reynolds number (Re), and the inlet

angle-of-yaw (γ) were set constant at 0.700, 4.0 x 10^6/ft and 0.0° respectively for this investigation. Table (3) displays the response variables for this study. They were the inlet total pressure recovery (PFAVE), the engine face distortion (DC60), and the first five Fourier harmonic 1/2 amplitudes (F1/2, F2/2, F3/2, F4/2, and F5/2) of engine face distortion.

The DOE strategy selected was a Central Composite Face-Centered (CCF) design plus a couple of additional experiments of special interest to the investigator. This strategy resulted in 54 unique experimental CFD cases for the "Taguchi" and "Higher Order" methodology, as indicated in Table (4), and 26 unique CFD cases for the "Lower Order" methodology as are shown in Table (5). In this example, the 26 CFD cases of the "Lower Order" design represent a subset of the "Taguchi" and "Higher Order" Central Composite Face-Centered (CCF) design. In general, this may not always be the case. Therefore, only 54 CFD cases were actually run in this study, the other set of 26 cases being a subset of the 54. Notice that these DOE cases covered a substantial range of possible flow situations over a wide range of angle-of-incidences from 0.0° to 20.0°. The DOE designs shown in Table (4) and (5), like most DOE strategies, varied more than one factor at a time. Further, this layout of 54 (or 26) cases permitted the estimation of both linear and curvilinear effects as well as interactive or synergistic effects among the DOE factors. This is very important in the study of secondary flow control since very strong interaction effects can develop between separate bands of micro-scale effectors. Since the Taguchi and "Higher Order" DOE approach repeated the basic CCF strategy of 26 cases at 0°, 10.0°, and 20.0° angle-of-incidence, the three way interactions involving α were also estimated. This CCF DOE strategy is superior to the traditional Edisonian approach where only changing one variable at a time does not permit the estimation of factor interactions. All three DOE approaches are more economical than a full factorial approach where the number of experiments would be 3^5 or 243 separate CFD cases. But most important, the "Lower Order" DOE approach at 26 runs is more economical than a comparable "Taguchi" and "Higher Order" approach requiring 54 runs in this particular example.

Each of the 54 cases in Table (4) were run with a Reynolds-averaged Navier-Stokes code[9] that allowed for numerical simulation of micro-vane effectors without the need to physically embed the vane effectors within the CFD grid structure. For the present study, however, the individual vanes were incorporated into the grid structure, and the appropriate boundary conditions applied to the individual effector vanes.The half-plane grid structure was composed of three blocks: an upstream block, a effector section containing the micro-vanes, and a downstream block. See Figures (3) and (4). The computational half-plane grid varied in total number of mesh points from about 750,00 to 1,500,000 depending on the micro-vane configuration. All CFD calculations were accomplished assuming half-plane symmetry. It was important to investigate the interactions between the separate effector bands without using the vane model in the code, so that proper band interaction could be established. This also established a set of baseline validation data to further verify the vane effector model in the Navier-Stokes code[9] for multi-band flow control design concepts.

To introduce an angle-of-incidence (α-disturbance) into the flow analysis, the condition was imposed that the initial station have an angle-of-incidence component that approximated the measured angle-of-incidence flow field[10]. Even though introducing an α-disturbance into the flow field is not rigorous, it provides a remarkably good approximation in comparison to the experimental flow field. The overall intent of introducing an α-disturbance into the flow field

in this manner was to economically determine the degree of tolerance of the MSFC installation design to angle-of-incidence.

Harmonic Analysis of Distortion

The overall methodology used to obtain the harmonic content of inlet distortion was first proposed by Ludwig[11] and is currently in use at the Williams International Corporation. This methodology is characterized by the use of radial weighting factors applied to the total pressure rake measurements. The radial weighting factors are shown in Table (6).These radial factors compress the rake information to a single radius ring of data samples, where the number of data samples corresponds to the number of arms of the measurement rake. A separate study was initiated by Anderson and Keller[6] to evaluate the impact of rake geometry (specifically the number of rake arms) on the measurement error associated with estimating the first five Fourier harmonic 1/2 amplitudes of engine face distortion. As a result of that study, the rake and methodology chosen for this study was the 80-probe clocked rake because it provided the lowest error in estimating the first five Fourier harmonic 1/2 amplitudes of engine face distortion. Using the AIP instrumentation locations for the 80-probe rake, the 54 CFD solutions were interpolated at each of the probe positions shown in Figure (5a). The span-weighted average total pressure was calculated for the 80-probe rake by multiplying the probe total pressure by the span-weighted coefficients from Table (6), and adding the results over the five probes of the rakes to form a single radius ring of data samples.

Since the rake at the engine face was "clocked", a complete set of "repeats" was generated at each experimental run in Tables (4) and (5). From the engine face patterns at each of the 10 clocking angles, a Fourier analysis was performed on the sample set of data and a standard deviation of the "repeats", S_{clock}, was determined for each of the Fourier harmonic 1/2 amplitudes. In order to check the constant variance assumption associated with standard least square regression, a simple F-test for comparing the minimum standard deviation to the maximum standard deviation ($F = S^2_{max}/S^2_{min}$) was conducted for each of the five responses. The results are presented in Table (7). Since each F-test exceeded the 95% confidence critical value of $F(0.975,9,9) = 4.03$, the assumption of constant variation across the design space had to be discarded. This meant that a regression technique known as weighted least squares regression had to be employed for analyzing the $10 \times 54 = 540$ separate engine face total pressure recovery patterns in the DOE. The weights in these regression analyses were set to $1/S^2_{clock}$.

The data reduction for the inlet total pressure recovery and engine face distortion differed greatly from the harmonic analysis of distortion described. Both the inlet total pressure recovery and engine face distortion were calculated directly from the computational grid at the engine face station. See Figure (5b). There is at present, no recognized technique for evaluating the Fourier harmonic 1/2 amplitudes for more than five probes in the radial direction. The engine face computational mesh was composed of 49 x 121 grid points in the full-plane. The DC60 engine face distortion descriptor[8] is defined such that it can be determined from either a computational grid or a standard measurement rake. It is the only recognized distortion descriptor that has this property, and hence, was chosen for this study. The DC60 engine face distortion descriptor is a distortion parameter commonly used throughout Europe and is usually determined from a 72-probe standard AIP rake.

Robust Design Methodologies

Taguchi *Robust Parameter Design* methodology - In the traditional Taguchi *Robust Parameter Design* methodology, a two tier experimentation strategy is used to solve the robust design problem. The control factors (design variables) are studied in their own DOE, called the inner array. A separate DOE, called the outer array, is constructed using only the environmental or noise variables. For each point in the inner array DOE, the entire outer array DOE is run and a Taguchi-style signal-to-noise ratio, S/N is calculated using the values from the outer (mission) array matrix. The S/N becomes the response that is analyzed over the controlled variables in the inner array. Therefore, the resulting regression model for S/N was a subset of the full quadric model permitted by the DOE and subsequent data analysis, namely:

$$S/N = \beta_0 + \beta_1 h_1 + \beta_2 h_2 + \beta_3 h_3 \quad \text{(linear effects of inner array variables)}$$
$$+\beta_{11} h_1^2 + \beta_{22} h_2^2 + \beta_{33} h_3^2 \quad \text{(quadratic effects of inner array variables)}$$
$$+\beta_{12} h_1 h_2 + \beta_{13} h_1 h_3 + \beta_{23} h_2 h_3 \quad \text{(interactive effects of inner array variables)}$$

Using the regression model, the S/N response is maximized/minimized to find the optimal settings for the inner array variables that produces the best response that is robust/insensitive to the outer array variables. Because the outer (mission) array matrix is run for every point in the inner design array DOE, the setup is called a product array. While a robust flow control installation can be established using the traditional Taguchi *Robust Parameter Design* methodology, the performance information of that installation over the outer array (mission) variable range is lost. This loss occurred as result of collapsing of the outer array mission matrix information, (i.e. the α-dependence), into the signal-to-noise parameter. Also, the traditional style Taguchi DOE is expensive. The total number of experiments is the product of the number of experiments in the inner array matrix times the number of experiments in the outer array matrix.

"Higher Order" Robust Methodology - An alternate method of analyzing the data from a traditional Taguchi DOE design is to not lose information by collapsing the outer array matrix information into a S/N, but to model the actual response data using an expanded regression model that includes the outer array variables directly Therefore, the resulting regression model for response Y in the "Higher Order" Robust methodology is a subset of the full quadratic and higher order interaction model permitted by the DOE, namely:

$$Y = \beta_0 + \beta_1 h_1 + \beta_2 h_2 + \beta_3 h_3 + \beta_4 \alpha \quad \text{(linear effects of inner array variables)}$$
$$+\beta_{11} h_1^2 + \beta_{22} h_2^2 + \beta_{33} h_3^2 + \beta_{44} \alpha^2 \quad \text{(quadratic effects of inner \& outer array variables)}$$
$$+\beta_{12} h_1 h_2 + \beta_{13} h_1 h_3 + \beta_{14} h_1 \alpha \quad \text{(interactive effects of inner \& outerarray variables)}$$
$$+\beta_{23} h_2 h_3 + \beta_{24} h_2 \alpha + \beta_{34} h_3 \alpha \quad \text{(interactive effects of inner \& outer array variables)}$$
$$+\beta_{114} h_1^2 \alpha + \beta_{224} h_2^2 \alpha + \beta_{334} h_3^2 \alpha \quad \text{(higher order interactions of inner \& outer variables)}$$
$$+\beta_{124} h_1 h_2 \alpha + \beta_{134} h_1 h_3 \alpha + \beta_{234} h_2 h_3 \alpha \quad \text{(higher order interactions of inner \& outer variables)}$$
$$+\beta_{144} h_1 \alpha^2 + \beta_{244} h_2 \alpha^2 + \beta_{344} h_3 \alpha^2 \quad \text{(higher order interactions of inner \& outer variables)}$$
$$+\beta_{1144} h_1^2 \alpha^2 + \beta_{2244} h_2^2 \alpha^2 \quad \text{(higher order interactions of inner \& outer variables)}$$

$+\beta_{3344}h_3^2\alpha^2+\beta_{1244}h_1h_2\alpha^2$ (higher order interactions of inner & outer variables)

$+\beta_{1344}h_1h_3\alpha^2+\beta_{2344}h_2h_3\alpha^2$ (higher order interactions of inner & outer variables)

While "Taguchi" *Robust Parameter Design* methodology contains the higher order interactive terms implicitly, the "Higher Order" methodology contains the higher order interactive terms explicitly in the regression model. To bring the desired robustness aspect into the design problem, the regression model was manipulated in a unique way during the data optimization phase. This is described in detail in the following section entitled "Flow Control Mission Studies".

"Lower Order" Robust Methodology - Cost saving can be achieved by a DOE in which the noise factors (mission variables) are introduced directly into the inner array design matrix with the controlled (design) variables. This is called a combined array format, which can have significant run-size savings over the traditional Taguchi robust design methods. Thus, in the new and economical approach to a Robust Design methodology, a single DOE is established composed of both the inner array (design) variables and outer array (mission) variables. At each point in the combined DOE, the responses are measured. Using weighted or ordinary least squares (OLS) regression, a model is built that is a function of both the inner array (design) variables and outer array (mission) variables. For the current study, the resulting regression model for each response was a subset of the full quadratic model permitted by the DOE, namely:

$Y = \beta_0 +\beta_1h_1 +\beta_2h_2 + \beta_3h_3 + \beta_4\alpha$ (linear effects of inner & outer array variables)

$+\beta_{11}h_1^2 + \beta_{22}h_2^2 +\beta_{33}h_3^2 + \beta_{44}\alpha^2$ (quadratic effects of inner & outer array variables)

$+\beta_{12}h_1h_2 + \beta_{13}h_1h_3 + \beta_{14}h_1\alpha$ (interactive effects of inner & outer array variables)

$+\beta_{23}h_2h_3 + \beta_{24}h_2\alpha + \beta_{34}h_3\alpha$ (interactive effects of inner & outer array variables)

To bring to fruition the desired robustness aspect of this study, this second order model in both the inner array and outer array was exploited in a unique way during the optimization phase. The robustness aspects are described in deal in the following section entitled "Flow Control Mission Studies".

Flow Control Mission Studies

To illustrate the potential of the three Robust Design methodologies, two mission strategies were considered for the subject inlet, namely (1) Maximum Performance, and (2) Maximum HCF Life Expectancy. The Maximum Performance mission sought to minimize the inlet duct losses (maximize the engine face total pressure recovery) subject to the constraint that the DC60 engine face distortion be less than 0.10, while no conditions were placed on the first five Fourier harmonic 1/2 amplitudes of distortion. A DC60 distortion level of 0.10 or less is significant because it would be acceptable for a commercial engine application. The Maximum HCF Life Expectancy mission sought to minimize the mean of the first five Fourier harmonic 1/2 amplitudes of distortion, also subject to the constraint that the DC60 engine face distortion be less than 0.10. In this mission, however, no constraint was placed upon the inlet total pressure recovery.

Maximum Performance Mission - For the "Optimal Robust" MSFC installation, the engine face distortion constraint DC60 $\leq$ 0.10 was imposed and a search was made over the design variable space to locate that installation geometry that maximized the optimization parameter $\Sigma Y_\alpha/m$ where Y_α = PFAVE at each of the $\alpha = 0^o$, 1.0^o,..., 20.0^o angle-of-incidences and m = 21. Again, for this mission no constraints were placed on the first five Fourier harmonic 1/2 amplitudes of engine face distortion. This procedure defined one installation that was "Optimal Robust" over the entire range of angle-of-incidence.

The "Optimal Robust" Maximum Performance installations and their corresponding CFD performance are presented in Tables (8), (9) and (10) and were determined through a search process to have the following effector vane heights (mm):

$h_1 = 0.0, h_2 = 0.0, h_3 = 1.90$	"Lower Order" Robust Methodology
$h_1 = 0.0, h_2 = 0.06, h_3 = 1.96$	Taguchi *Robust Parameter Design* Methodology
$h_1 = 0.0, h_2 = 0.09, h_3 = 1.90$	"Higher Order" Robust Methodology

The inlet CFD validation engine total pressure recoveries contours solution for the "Optimal Robust" Maximum Performance installations design at the engine face is presented in Figure (6), (7) and (8). Note that the optimal factor vane heights are not very different for each of the Robust methodologies studied, and the performance that is achieved with these factor values are essentially the same. The CFD validation of the optimally determined DOE factors combination all satisfy the mission objectives. It is important to note that all the Robust design mythologies studied provide excellent installation designs, but that the "Lower Order" Robust methodology was far more economical and required the least computational effort.

The near wall streamlines for the baseline solution and the "Optimal Robust" Maximum Performance installation designs are presented in Figures (9), (10), (11) and (12). A comparison of these figures indicates the underlying operational purpose of micro-scale secondary flow control. In the baseline case presented in Figure (9), the flow in a very thin layer adjacent to the walls "over turns" as a result of a loss of momentum within the inlet boundary layer. Eventually, this "over-turning" will cause a vortex pair to form in the inlet passage. This vortex pair results in total pressure loss and severe total pressure distortion at the engine face. It is not necessary for this vortex to "lift-off" or separate from the walls for high total pressure loss and distortion to occur (hence the terminology inlet "secondary flow control" rather than "separation control"). By introducing the micro-effectors into the inlet, whether vanes or jets, the "over-turning" in the inlet boundary is prevented. See Figure (10), (11) and (12). Consequently, the passage vortex will not form or, at worst, is greatly reduced in strength, which will result in a vast improvement in engine face distortion. Therefore, the entire inlet flow field can be managed by controlling the secondary flow in a thin layer adjacent to the inlet walls. In the MSFC concept, micro-scale actuation is used as an approach called "secondary flow control" to alter the S-duct's inherent secondary flow characteristics with the goal of simultaneously improving the critical system level performance metrics pressure recovery, engine face distortion, and HCF characteristics.

Presented in Figures (13a) through (13h) are a comparison of the Maximum Performance optimal Robust angle-of-incidence performance for the Taguchi *Robust Parameter Design* methodology, the "Lower Order" Robust method, and the "Higher Order" Robust methodology. The response parameters for this comparison were the inlet pressure recovery (PFAVE), the engine face distortion (DC60), the first five Fourier harmonic 1/2 amplitudes of distortion (F1/2,

F2/2, F3/2, F4.2, F5/2), and the mean of the first five Fourier harmonic 1/2 amplitudes (FM/2). In order to obtain the angle-of-incidence performance for the Taguchi optimal MSFC installation design, it was assumed that the regression for the "Higher Order" methodology was valid for the Taguchi installation design. Therefore, to recover the performance information for the optimal Taguchi installation design over the mission variable range required considerable effort over and above the traditional Taguchi approach. Both the Taguchi and "Higher Order" optimal angle-of-incidence performance included the higher order interactions among the DOE variables. The "Lower Order" Robust methodology included the two-way interaction and quadratic terms, but not the higher order interaction DOE terms. Therefore, the differences that appeared among the Robust methodologies in Figures (13a) through (13h) resulted primarily from the different regression models used in determining the angle-of-incidence performance for the three optimal MSFC installation designs. Visually comparing the Taguchi and "Higher Order" optimal installation performance for all responses indicates essentially the same performance. The performance for engine face recovery (PFAVE) and distortion (DC60) were essentially the same for all the Robust methodologies. These are the two critical parameters in inlet design because they affect aircraft performance and engine stability during flight. The differences that appeared among the three methodologies were manifested in the first five Fourier harmonic 1/2 amplitudes were fortunately were "small". They did not appreciably effect the selection of the optimal installation design. See Tables (8), (9) and (10). The CFD validation of all the optimally determined installation designs all satisfied the mission objectives.

Maximum HCF Life Expectancy Mission - For the "Optimal Robust" Maximum HCF Life Expectancy MSFC installation, the engine face distortion constraint, DC60 ≤ 0.10, was imposed and a search was made over the design variable space to locate that installation geometry that minimized $\Sigma Y_\alpha/m$, where $Y_\alpha = \Sigma Fj/5$, (the mean of the first five Fourier harmonic 1/2 amplitudes present in the engine face distortion), where $\alpha = 0^o, 1.0^o, ..., 20.0^o$.

The "Optimal Robust" Maximum HCF Life Expectancy installations and their corresponding CFD performance are presented in Tables (11), (12) and (13) and were determined to have the following effector vane heights (mm):

$h_1 = 0.0, h_2 = 0.0, h_3 = 2.00$	"Lower Order" Robust Methodology
$h_1 = 0.0, h_2 = 0.52, h_3 = 2.00$	Taguchi *Robust Parameter Design* Methodology
$h_1 = 0.0, h_2 = 0.40, h_3 = 1.90$	"Higher Order" Robust Methodology

These optimal factor values were determined through a search process over the design parameter space, whose boundaries were defined by the original DOE. See Tables (4) and (5). Notice that the optimal Taguchi and "Higher Order" installation optimal factor combinations are essentially the same, but differ from the "Lower Order" optimal installation design by the inclusion of a finite h_2 band of micro-vane effectors. This difference arose because of the higher order interactions contained in the Taguchi and "Higher Order" models. The inlet CFD engine total pressure recoveries contours solution for the "Optimal Robust" Maximum HCF Life Expectancy installation designs at the engine face are presented in Figure (14), (15) and (16). Although the optimal factor vane heights are somewhat different for each of the Robust methodologies studied, the ultimate performance that is achieved with these factor values are essentially the same, certainly within the margin of error that can be measured in wind tunnel experiments with standard 40-probe rakes.

Presented in Figure (17) is the near wall streamlines for the baseline duct at 0° angle-of-incidence. Figures (18), (19), and (20) present the "Optimal Robust" Maximum HCF Life Expectancy installation designs for the three Robust methodologies, also at $\alpha = 0.0°$. Again, notice the effect of the micro-vane effectors in preventing the over-turning of the flow adjacent to the inlet walls and thus suppressing the passage vortex formation. Once again, there was a vast improvement in engine face distortion.

Presented in Figures (21a) through (21h) are a comparison of the Maximum HCF Life Expectancy optimal angle-of-incidence performance for the Taguchi *Robust Parameter Design* methodology, the "Lower Order" Robust method, and the "Higher Order" Robust methodology. The response parameters for this comparison were the inlet pressure recovery (PFAVE), the engine face distortion (DC60), the first five Fourier harmonic 1/2 amplitudes of distortion (F1/2, F2/2, F3/2, F4.2, F5/2), and the mean of the first five Fourier harmonic 1/2 amplitudes (FM/2). Similar type performance behavior occurred between the Robust methodologies as were determined for the Maximum Performance mission, except for the engine face recovery angle-of-incidence characteristics, where the PFAVE distribution for the Taguchi installation was about 0.025 higher than the other design methods. See Figure (21a). Again, the engine face distortion (DC60) angle-of-incidence performances were essentially the same for all the Robust methods. While differences among the three Robust methodologies can be seen for the first five Fourier harmonic 1/2 amplitudes of distortion, Figure (21c) through (21g), these differences were primarily caused by the different regression models used in the DOE performance predictions. The CFD validation of the optimally determined Maximum HCF Life Expectancy installation designs all satisfied the mission objectives. Again, the CFD performances were essentially the same for all the optimal determined designs when independently tested during the CFD validation phase of the study. See Tables (11), (12) and (13).

Statistical Comparison of CFD Analysis and DOE Predictions

Extensive CFD validation cases were included in this study and these are presented in Tables (14) and (15). Table (14) defines the CFD validation installation geometries and conditions evaluated. This evaluation covered the Maximum Performance and Maximum HCF Life Expectancy missions, and the three Robust methodologies evaluated each at 0°, 10.0°, and 20.0° angle-of-incidence. There were a total of 18 CFD validation cases. They represent the six optimal robust installation geometries determined by the respective three Robust methodologies. The CFD validation performance results for each of these 18 test cases are presented in Table (15), and included all the response variables important for this study, i.e. inlet pressure recovery (PFAVE), engine face distortion (DC60), and the first five Fourier harmonic 1/2 amplitudes of distortion (F1/2, F2/2, F3/2, F4/2, and F5/2). A direct statistical comparison be made between the optimal responses predicted by the DOE models (Y_{DOE}) with the actual CFD predicted performance values (Y_{CFD}) through the expression:

$$t^* = \frac{\left|\ln(Y_{CFD}) - \ln(Y_{DOE})\right|}{\dfrac{\ln(Y_A) - \ln(Y_{DOE})}{t(0.975, N-p)}} \quad (1)$$

where Y_A is the upper 95% confidence interval for the individual predicted response Y_{DOE} from the regression model, and t(0.975,N-p) is the 95% confidence t-value for N-p degrees of freedom. Since all the response parameters except for PFAVE were modelled under a natural log transformation, the natural log of the response (Y) had to be used, i.e. ln(Y), for those responses. For a statistically significant difference to exist between the DOE model predicted response (Y_{DOE}) and the CFD validation response prediction (Y_{CFD}), the expression:

$$t^* > t(0.975, N-p) \quad (2)$$

must hold. Likewise, if the expression

$$t^* < t(0.975, N-p) \quad (3)$$

is valid, the Y_{CFD} is not statistically different from Y_{DOE}. Therefore, for no significant statistical difference to exist between the DOE model predicted response Y_{DOE} and the CFD analysis response Y_{CFD}, the CFD response prediction must fall within the 95% confidence interval of the DOE model prediction for that response. In each case, the comparison was made with the optimal Robust installation. See Tables (14) and (15). Tables (16) through (21) show the results of this statistical comparison over the range of optimal installations, missions, Robust methodologies, and angle-of-incidences from 0° to 20.0.° In general, the number of incidences when the comparisons were statistically different was about 5%, which is remarkably good This indicates that the optimal installations determined by the DOE models were a statistically valid optima when compared to the actual CFD installation analysis.

Statistical Comparison of Robust Design Methodologies

This study involves the statistical comparison of two DOE model predicted response values Y_i and Y_j from two different regression models (i) and (j) at two different optimal factor combinations X_i and X_j. Again, since all the responses except PFAVE were conducted using a natural log transformation, all the responses (except PFAVE) were considered as $\ln(Y_i)$ and $\ln(Y_j)$. A direct statistical comparison can be made between the optimal response Y_i predicted by the DOE model (i) having optimal factor combinations X_i, with the response Y_j predicted by DOE model (j) having optimal factor combinations X_j through the expression:

$$t^* = \frac{\left|\ln(Y_i) - \ln(Y_j)\right|}{\sqrt{\left(\frac{\ln(Y_A) - \ln(Y_i)}{t(0.975, N-p)}\right)^2 + \left(\frac{\ln(Y_B) - \ln(Y_j)}{t(0.975, N-p)}\right)^2}} \quad (4)$$

where Y_A is the upper 95% confidence interval for the individual response Y_i from DOE model (i), Y_B is the upper 95% confidence interval for the individual response Y_j from DOE model (j), and t(0.975,N-p) is the 95% confidence t-value for N-p degrees of freedom in error. For a statisti-

cally significant difference to exist between the DOE model (i) predicted response (Y_i) and the DOE model (j) predicted response (Y_j), the expression:

$$t^* > t(0.975, N - p) \qquad (5)$$

must be hold. Likewise, if the expression

$$t^* < t(0.975, N - p) \qquad (6)$$

is valid, the Y_i is not statistically different from Y_j. The statistical comparison between the DOE Robust methodologies are presented is Tables (22) through (27), for both the Maximum Performance and Maximum HCF Life Expectancy missions. No statistical difference was found to exist between the Taguchi and "Higher Order" Robust methodologies at the optimal Robust installation designs, Tables (22) and (25). However, statistical differences were found when comparing the "Lower Order" with both the Taguchi and "Higher Order" Robust methodologies and these difference occurred in approximately 5% to 7% of the comparisons. See Tables (22), (24), (25) and (27).

CONCLUSIONS

The fundamental importance of Genichi Taguchi's contribution to *Total Quality Design* over traditional design approaches lies in the idea that process and product variability can be incorporated into the optimal statistical Design-of-Experiment and subsequent analysis of data. To the aerodynamicist, it represents a major breakthrough in the area of aerodynamic design of inlets, since the effect of the mission variables can be directly introduced into the design process. The inlet system can now be designed to operate with optimal performance over a range of specified mission variables.Taguchi's *Robust Parameter Design* method, however, may not be optimal in the design of secondary flow installations for inlet systems because: (a) it loses information vital to the aerodynamicist and, (b) it is costly. Fortunately, the important aspects surrounding Taguchi's approach to *Robust Parameter Design* can and have been incorporated into an alternate economical approach and adapted to the inlet design problem.

In this report, three Robust optimal design methodologies were studied and evaluated. These include (1) the traditional Taguchi *Robust Parameter Design* methodology, (2) a "Higher Order" Robust method, which used the same DOE structure as Taguchi, but with an alternate analysis which does not lose information by collapsing the outer array matrix information into a S/N parameter, and (3) a "Lower Order" economical approach to Robust Design, where a single DOE was established which was composed of both the inner array (design) variables and outer array (mission) variables. For each of the three Robust design methodologies, two different mission strategies were considered for the subject inlet, namely (1) Maximum Performance, and (2) Maximum HCF Life Expectancy. The Maximum Performance mission maximized total pressure recovery while the Maximum HCF Life Expectancy mission minimized the mean of the first five Fourier harmonic 1/2 amplitudes, i.e. "collectively" reduced all the Fourier harmonic 1/2 amplitudes of engine face distortion. Each of the mission strategies was subject to a low engine face distortion constraint, i.e. DC60 $\leq$ 0.10, which is a level acceptable for commercial engines.

The angle-of incidence range was the Taguchi noise or environmental variable over which each optimal installations had to be robust.

Each of the three Robust methodologies examined in this report, (i.e. the Taguchi methodology, the "Higher Order" methodology, and the "Lower Order" methodology) provided installation designs that satisfied the two mission requirements. The two mission requirements were Maximum Performance and the Maximum HCF Life Expectancy objectives. For each of the six optimal Robust installation designs (i.e. the three methodologies and two mission strategies), the DOE model predicted performance were successfully validated with CFD verification runs (i.e. no substantial differences were found between the DOE model predictions and CFD validation results). Also, statistical comparison among the Optimal Robust performance of the three Robust methodologies indicated no significant differences between the Taguchi and the "Higher Order" methodologies and only minor differences between the "Lower Order" and the "Higher Order" and the Taguchi methodologies. This was true for both mission strategies. The slight differences in final Robust Optimal performance were negligible when compare the differences that would be discernible in a Wind Tunnel experiment. Hence, even though all three methodologies were capable of finding a robust optima that satisfied the mission requirements, the "Lower Order" method provides an economical alternative where the number of runs is drastically reduced.

REFERENCES

(1) Anderson, B. H., Miller, D. M., Yagel, P. J, and Traux, P. P., "A Study of MEMS Flow Control for the Management of Engine Face Distortion in Compact Inlet Systems", FEDSM99-6920, 3rd ASME/JSME Joint Fluids Engineering Conference, San Francisco, CA, July 18-23, 1999.

(2) Hamstra, J. W., Miller, D. N., Truax, P. P., Anderson, B. H., and Wendt, B. J., "Active Inlet Flow Control Technology Demonstration", ICAS-2000-6.11.2, 22nd International Congress of the Aeronautical Sciences, Harrogate, UK, August 27th-September 1st, 2000.

(3) Taguchi, G and Wu, Y, "Introduction to Off-Line Quality Control," Central Quality Control Association, 1980.

(4) Anderson, B. H. and Keller, D. J., "Optimal Micro-Scale Secondary Flow Control for the Management of HCF and Distortion in Compact Inlet Diffusers", Proposed NASA TM, 2001.

(5) Anderson, B. H. and Keller, D. J., "A Robust Design Methodology for Optimal Micro-Scale Secondary Flow Control in Compact Inlet Diffusers", AIAA 2002-0000, Jan. 2002.

(6) Anderson, B. H. and Keller, D. J., "Considerations in the Measurements of Engine Face Distortion for High Cycle Fatigue in Compact Inlet Diffusers", Proposed NASA TM, 2001.

(7) Willmer, A. C., Brown, T. W. and Goldsmith, E. L., "Effects of Intake Geometry on Circular Pitot Intake Performance at Zero and Low Forward Speeds", Aerodynamics of Power Plant Installation, AGARD CP301, Paper 5, Toulouse, France, May 1981, pp 51-56.

(8) Goldsmith, E. L. and Seddon, J. (eds), "Practical Intake Aerodynamics," Blackwell Scientific Publications, Oxford, 1993.

(9) Bender, E. E, Anderson, B. H., and Yagle, P. J., "Vortex Generator Modeling for Navier Stokes Code", FEDSM99-69219, 3rd ASME/JSME Joint Fluids Engineering Conference, San Francisco, CA, July 18-23, 1999.

(10) Gibb, J. and Anderson, B. H., "Vortex Flow Control Applied to Aircraft Intake Ducts," Proceedings of the Royal Aeronautical Society Conf., High Lift and Separation Control, Paper No. 14, Bath, UK, March, 1995.

(11) Ludwig, G. R., "Aeroelastic Considerations in the Measurement of Inlet Distortion", 3rd National Turbine Engine High Cycle Fatigue Conference, 1998.

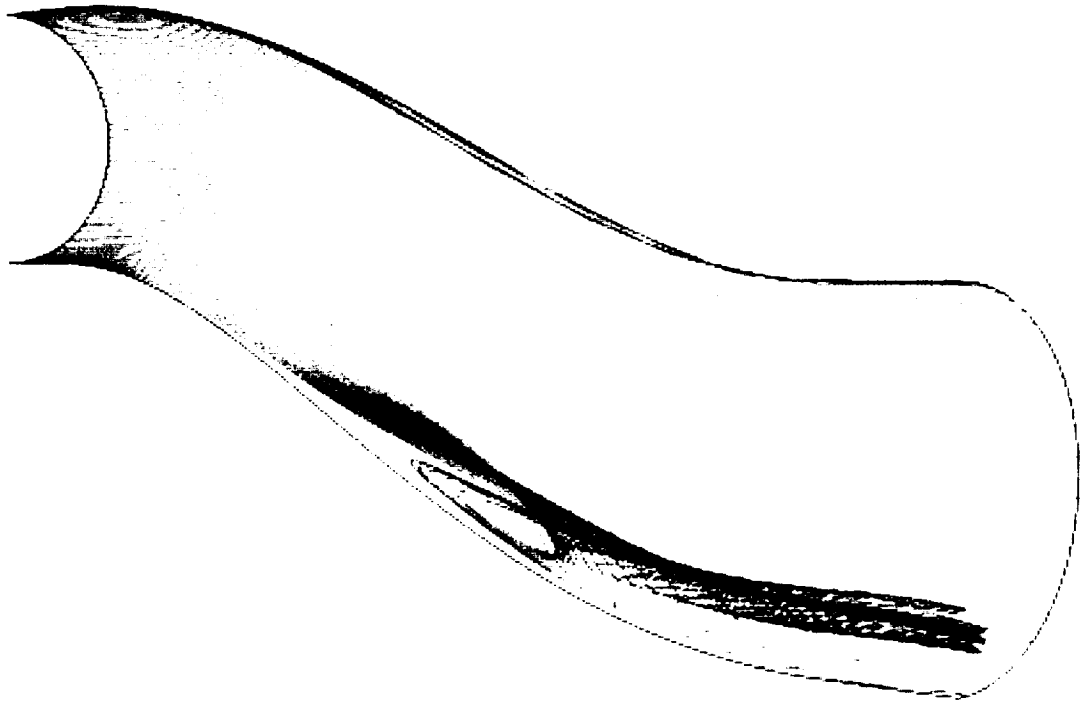

Figure (1): Particles traces showing the vortex liftoff (separation) within the DERA/M2129 inlet S-duct, Re = 4.0 x 10^6/ft., $\alpha = 0.0^o$.

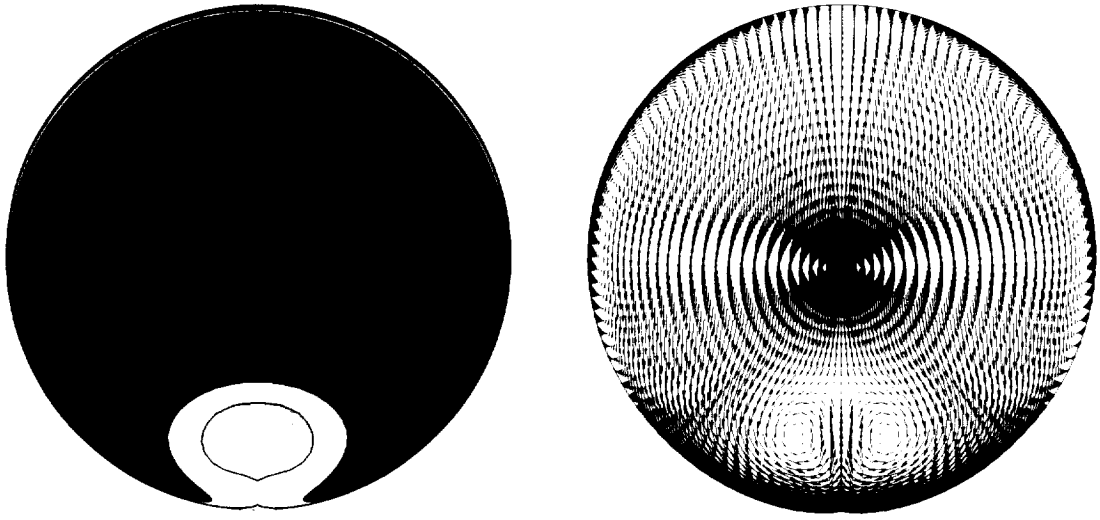

(a) Total Pressure Recovery Contours **(b) Secondary Flow Velocity Vectors**

Figure (2): Baseline engine face solution Re = 4.0 x 10^6/ft., $\alpha = 0.0^o$.

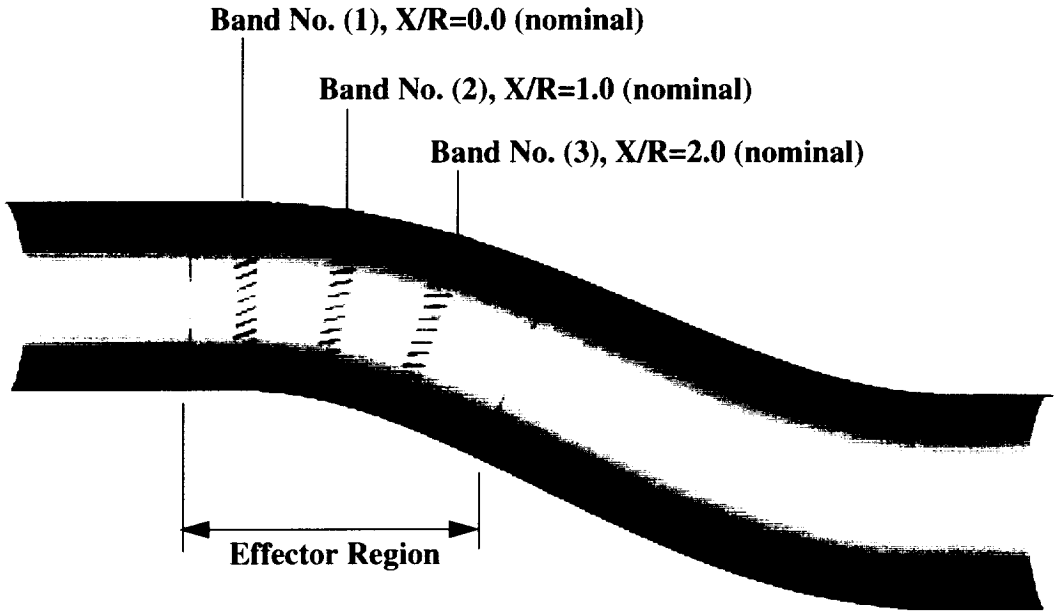

Figure (3): Location of effector region within the DERA/M2129 inlet S-duct.

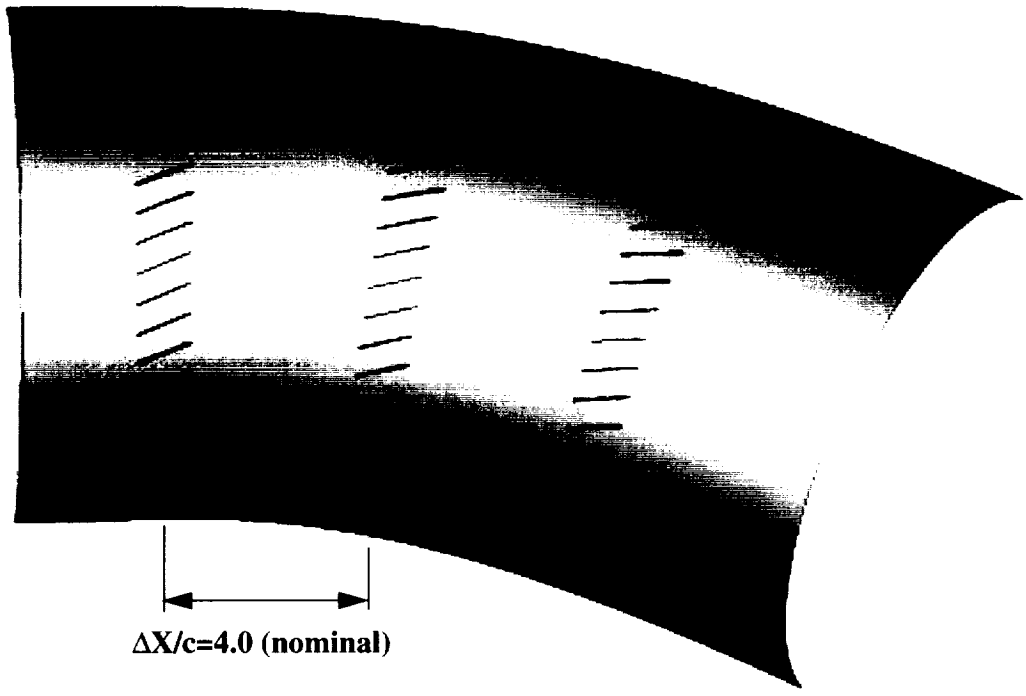

Figure (4): Micro-scale vane effector arrangement within effector region.

Factors	Range
Installation Vane Height (mm), h_1	0.0 to 2.0
Installation Vane Height (mm), h_2	0.0 to 2.0
Installation Vane Height (mm), h_3	0.0 to 2.0
Inlet Angle-of-Incidence, (degs.), α	0.0^o to 20.0^o

Table (1): Factors which establish the DOE design matrix.

Variable	Value
Number of Effectors Units, $n_{i,\ i=1,3}$	24
Vane Angle-of-Incidence, (degs.), $\beta_{i,\ i=1,3}$	24.0^o
Installation Chord Length (mm), $c_{1,\ i=1,3}$	16.0
Throat Mach Number, Mt	0.700
Reynolds Number, $x10^6$ /ft.	4.0
Inlet Angle-of-Yaw, (degs.), γ	0.0^o

Table (2): Variables held constant.

Design Responses	Nomenclature
Engine Face Total Pressure Recovery	PFAVE
Engine Face Distortion	DC60
1st Fourier Harmonic 1/2 Amplitude	F1/2
2nd Fourier Harmonic 1/2 Amplitude	F2/2
3rd Fourier Harmonic 1/2 Amplitude	F3/2
4th Fourier Harmonic 1/2 Amplitude	F4/2
5th Fourier Harmonic 1/2 Amplitude	F5/2

Table (3): DOE design responses.

Config.	h_1	h_2	h_3	α
nvg501	0.0	0.0	0.0	0.0
nvg502	2.0	0.0	0.0	0.0
nvg503	0.0	2.0	0.0	0.0
nvg504	2.0	2.0	0.0	0.0
nvg505	0.0	0.0	2.0	0.0
nvg506	2.0	0.0	2.0	0.0
nvg507	0.0	2.0	2.0	0.0
nvg508	2.0	2.0	2.0	0.0
nvg509	0.0	1.0	1.0	0.0
nvg510	2.0	1.0	1.0	0.0
nvg511	1.0	0.0	1.0	0.0
nvg512	1.0	2.0	1.0	0.0
nvg513	1.0	1.0	0.0	0.0
nvg514	1.0	1.0	2.0	0.0
nvg515	1.0	1.0	1.0	0.0
nvg516	1.0	0.0	0.0	0.0
nvg517	0.0	1.0	0.0	0.0
nvg518	0.0	0.0	1.0	0.0
nvg519	0.0	0.0	0.0	10.0
nvg520	2.0	0.0	0.0	10.0
nvg521	0.0	2.0	0.0	10.0
nvg522	2.0	2.0	0.0	10.0
nvg523	0.0	0.0	2.0	10.0
nvg524	2.0	0.0	2.0	10.0
nvg525	0.0	2.0	2.0	10.0
nvg526	2.0	2.0	2.0	10.0
nvg527	0.0	1.0	1.0	10.0

Table (4): Central Composite Face-Centered design (plus three additional cases), "Taguchi" and "Higher Order" Robust Design methodology.

Config.	h_1	h_2	h_3	α
nvg528	2.0	1.0	1.0	10.0
nvg529	1.0	0.0	1.0	10.0
nvg530	1.0	2.0	1.0	10.0
nvg531	1.0	1.0	0.0	10.0
nvg532	1.0	1.0	2.0	10.0
nvg533	1.0	1.0	1.0	10.0
nvg534	1.0	0.0	0.0	10.0
nvg535	0.0	1.0	0.0	10.0
nvg536	0.0	0.0	1.0	10.0
nvg537	0.0	0.0	0.0	20.0
nvg538	2.0	0.0	0.0	20.0
nvg539	0.0	2.0	0.0	20.0
nvg540	2.0	2.0	0.0	20.0
nvg541	0.0	0.0	2.0	20.0
nvg542	2.0	0.0	2.0	20.0
nvg543	0.0	2.0	2.0	20.0
nvg544	2.0	2.0	2.0	20.0
nvg545	0.0	1.0	1.0	20.0
nvg546	2.0	1.0	1.0	20.0
nvg547	1.0	0.0	1.0	20.0
nvg548	1.0	2.0	1.0	20.0
nvg549	1.0	1.0	0.0	20.0
nvg550	1.0	1.0	2.0	20.0
nvg551	1.0	1.0	1.0	20.0
nvg552	1.0	0.0	0.0	20.0
nvg553	0.0	1.0	0.0	20.0
nvg554	0.0	0.0	1.0	20.0

Table (4): Central Composite Face-Centered design (plus three additional cases), "Taguchi" and "Higher Order" Robust Design methodology, continued.

Config.	h_1	h_2	h_3	α
nvg501	0.0	0.0	0.0	0.0
nvg502	2.0	0.0	0.0	0.0
nvg503	0.0	2.0	0.0	0.0
nvg504	2.0	2.0	0.0	0.0
nvg505	0.0	0.0	2.0	0.0
nvg506	2.0	0.0	2.0	0.0
nvg507	0.0	2.0	2.0	0.0
nvg508	2.0	2.0	2.0	0.0
nvg537	0.0	0.0	0.0	20.0
nvg529	2.0	0.0	0.0	20.0
nvg530	0.0	2.0	0.0	20.0
nvg531	2.0	2.0	0.0	20.0
nvg532	0.0	0.0	2.0	20.0
nvg515	2.0	0.0	2.0	20.0
nvg551	0.0	2.0	2.0	20.0
nvg533	2.0	2.0	2.0	20.0
nvg519	0.0	1.0	1.0	10.0
nvg501	2.0	1.0	1.0	10.0
nvg502	1.0	0.0	1.0	10.0
nvg503	1.0	2.0	1.0	10.0
nvg504	1.0	1.0	0.0	10.0
nvg505	1.0	1.0	2.0	10.0
nvg506	1.0	1.0	1.0	0.0
nvg507	1.0	1.0	1.0	20.0
nvg508	1.0	1.0	1.0	10.0
nvg537	0.0	0.0	0.0	10.0

Table (5): Central Composite Face-Centered design (plus one additional case), "Lower Order" Robust Design methodology.

Ring Number	Radial Weighting Coefficient
1	0.05651
2	0.14248
3	0.21077
4	0.26918
5	0.32106

Table (6): Radial weighting coefficients applied to the total pressure rake measurements.

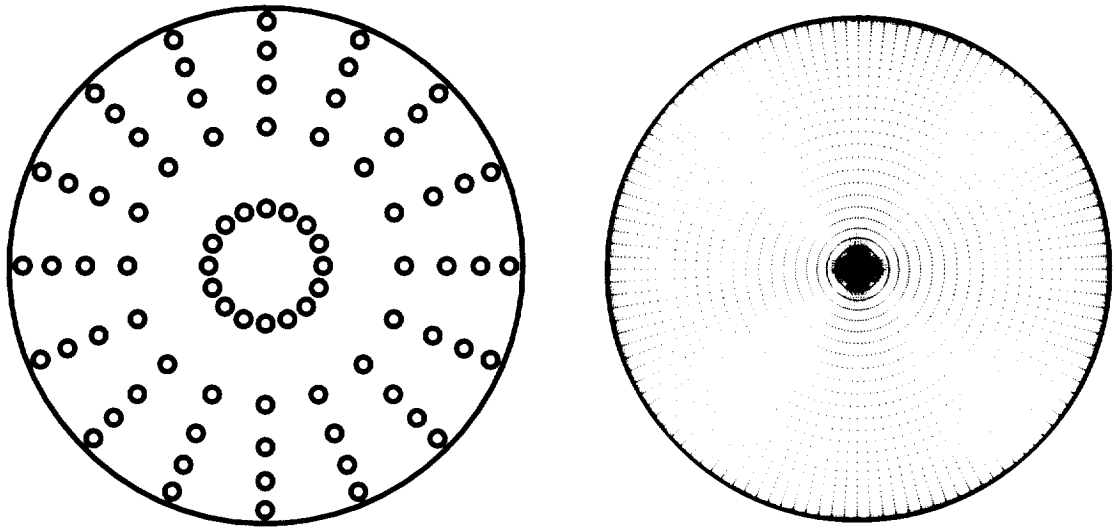

(a) 80-probe rake **(b) Computational grid**

Figure (5): Total pressure and distortion measurement arrays.

Response	Nomenclature	S^2_{max}/S^2_{min}	t(0.95,9,9)
1st Harmonic 1/2 Amplitude	F1/2	1939.9	4.03
2nd Harmonic 1/2 Amplitude	F2/2	53.5	4.03
3rd Harmonic 1/2 Amplitude	F3/2	160.0	4.03
4th Harmonic 1/2 Amplitude	F4/2	135.4	4.03
5th Harmonic 1/2 Amplitude	F5/2	47.6	4.03

Table (7): Fourier Harmonic 1/2 amplitude F-test compliance.

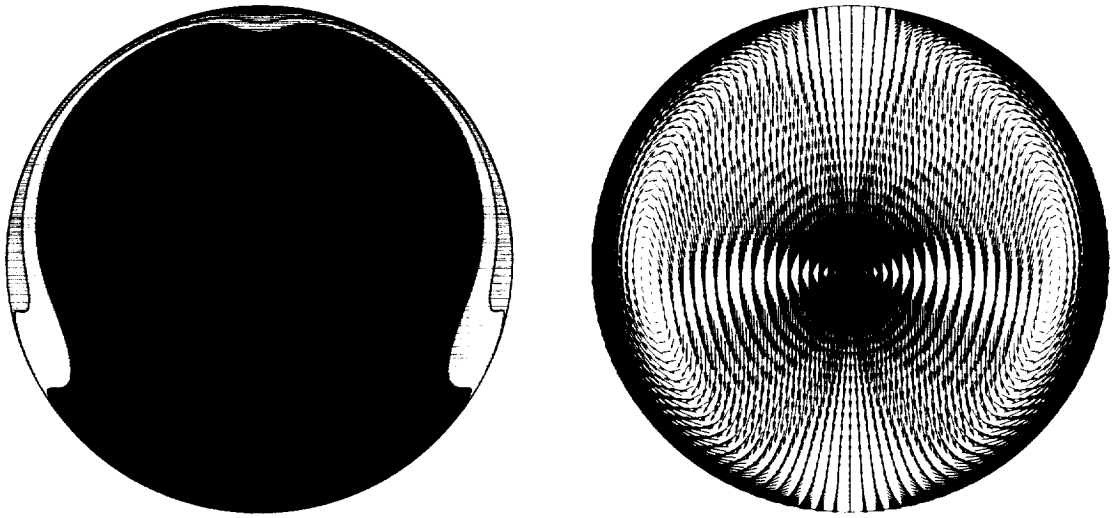

(a) Total pressure recovery contours (b) Secondary flow velocity vectors

Figure (6): Maximum Performance "Lower Order Robust" installation engine face CFD solution, $\alpha = 0.0^{o}$.

Factor/Response	Range/Constraint	Optimal Value
h_1	0.0 to 2.0	0.0
h_2	0.0 to 2.0	0.0
h_3	0.0 to 2.0	1.90
PFAVE	Maximized	0.97329
DC60	≤ 0.10	0.08401
F1/2	Unconstrained	0.00705
F2/2	Unconstrained	0.01636
F3/2	Unconstrained	0.01651
F4/2	Unconstrained	0.00527
F5/2	Unconstrained	0.00106
FM/2	Unconstrained	0.00925

Table (8): Maximum Performance "Lower Order Robust" installation inlet CFD performance, $\alpha = 0.0^{o}$.

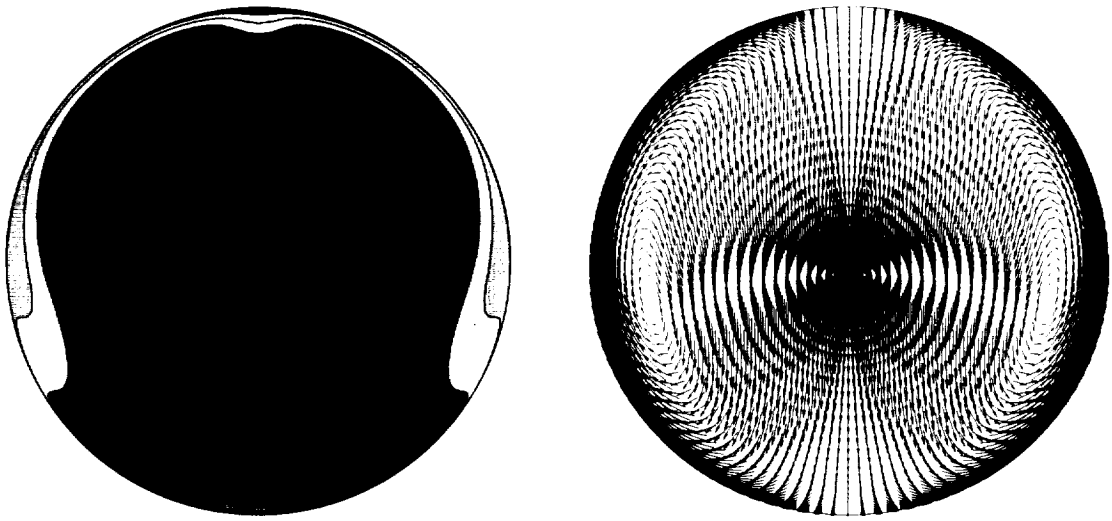

(a) Total pressure recovery contours (b) Secondary flow velocity vectors

Figure (7): Maximum Performance "Taguchi Robust" installation engine face CFD solution, $\alpha = 0.0^{o}$.

Factor/Response	Range/Constraint	Optimal Value
h_1	0.0 to 2.0	0.0
h_2	0.0 to 2.0	0.06
h_3	0.0 to 2.0	1.96
PFAVE	Maximized	0.97379
DC60	≤ 0.10	0.08582
F1/2	Unconstrained	0.00868
F2/2	Unconstrained	0.01757
F3/2	Unconstrained	0.01564
F4/2	Unconstrained	0.00498
F5/2	Unconstrained	0.00077
FM/2	Unconstrained	0.00953

Table (9): Maximum Performance "Taguchi Robust" installation inlet CFD performance, $\alpha = 0.0^{o}$.

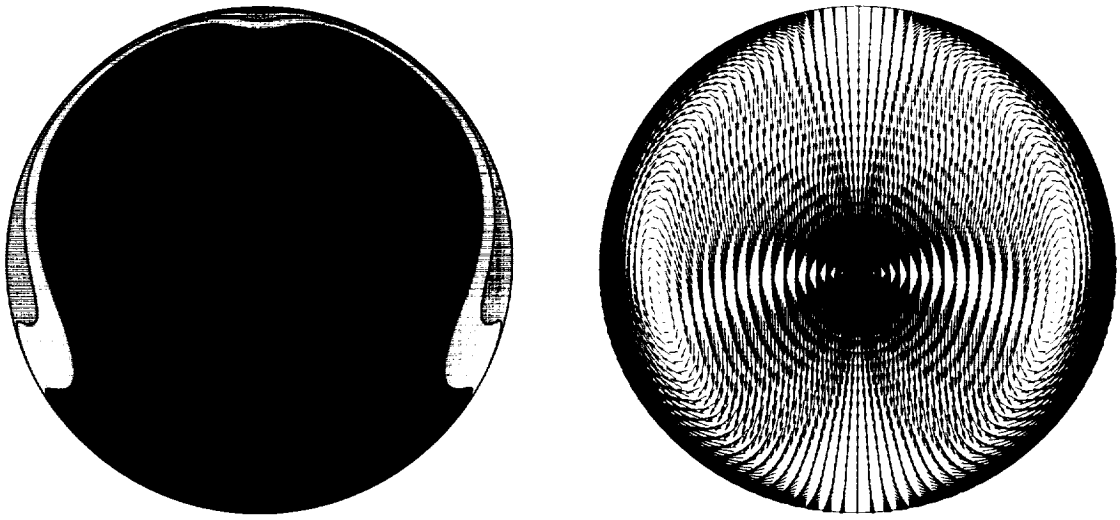

(a) Total pressure recovery contours (b) Secondary flow velocity vectors

Figure (8): Maximum Performance "Higher Order Robust" installation engine face CFD solution, $\alpha = 0.0^{o}$.

Factor/Response	Range/Constraint	Optimal Value
h_1	0.0 to 2.0	0.0
h_2	0.0 to 2.0	0.09
h_3	0.0 to 2.0	1.90
PFAVE	Maximized	0.97398
DC60	≤ 0.10	0.08570
F1/2	Unconstrained	0.00740
F2/2	Unconstrained	0.01683
F3/2	Unconstrained	0.01634
F4/2	Unconstrained	0.00520
F5/2	Unconstrained	0.00078
FM/2	Unconstrained	0.01072

Table (10): Maximum Performance "Higher Order Robust" installation inlet CFD performance, $\alpha = 0.0^{o}$.

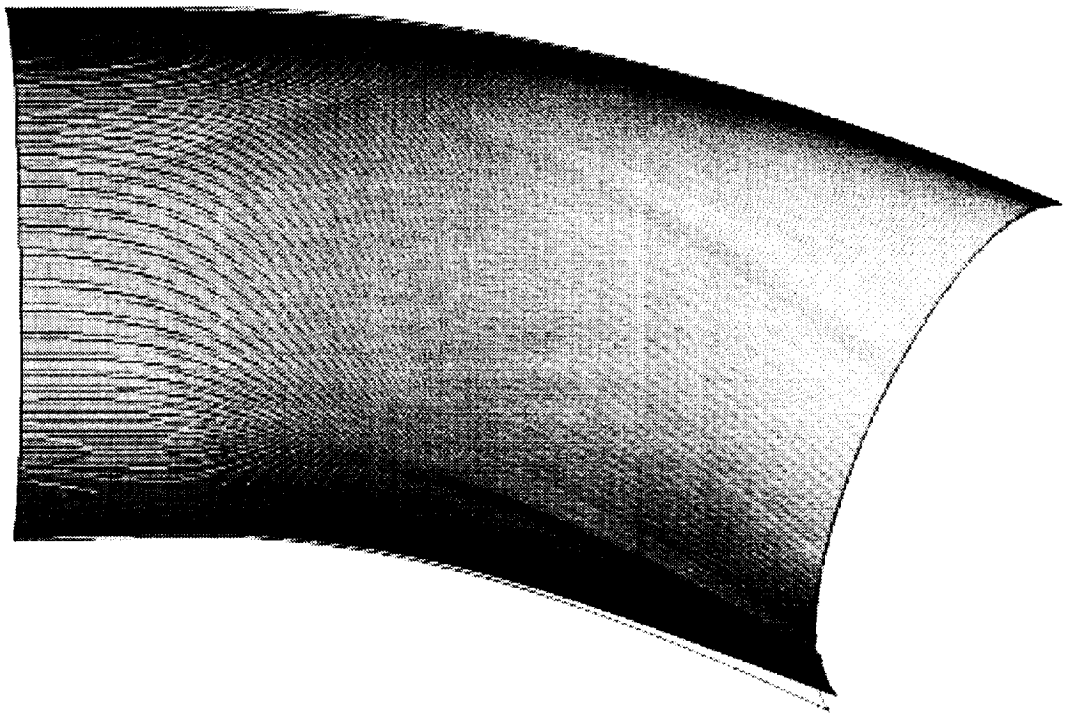

Figure (9): Near wall streamlines within effector region, baseline CFD solution, $\alpha = 0.0^{o}$.

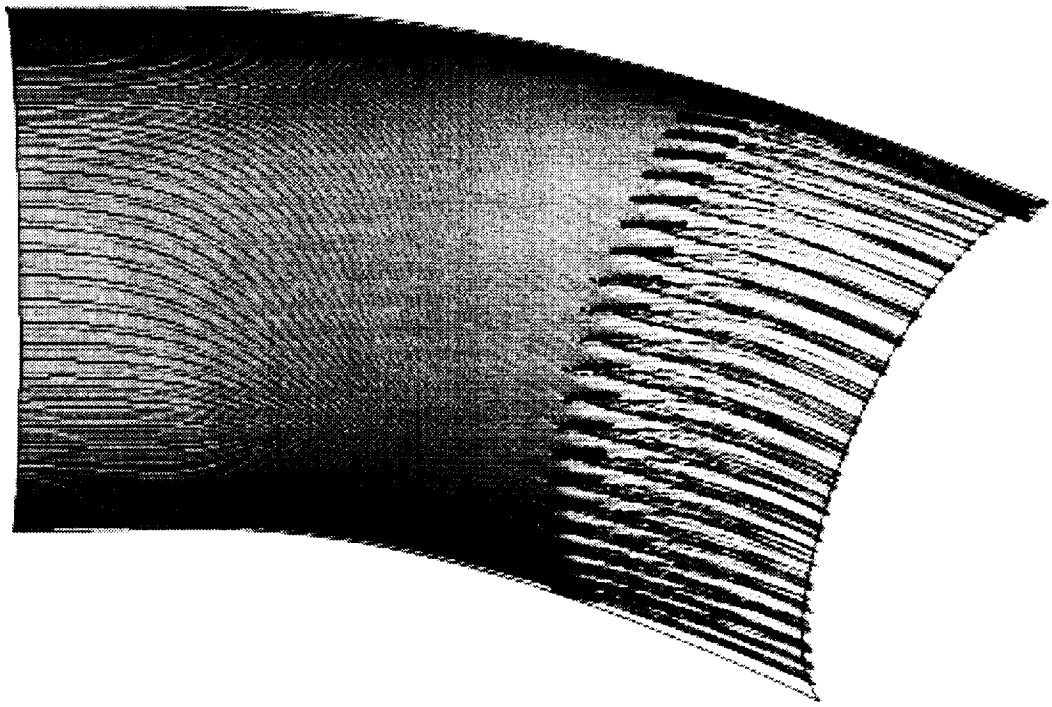

Figure (10): Near wall streamlines within effector region, Maximum Performance "Lower Order Robust" installation design, $\alpha = 0.0^{o}$.

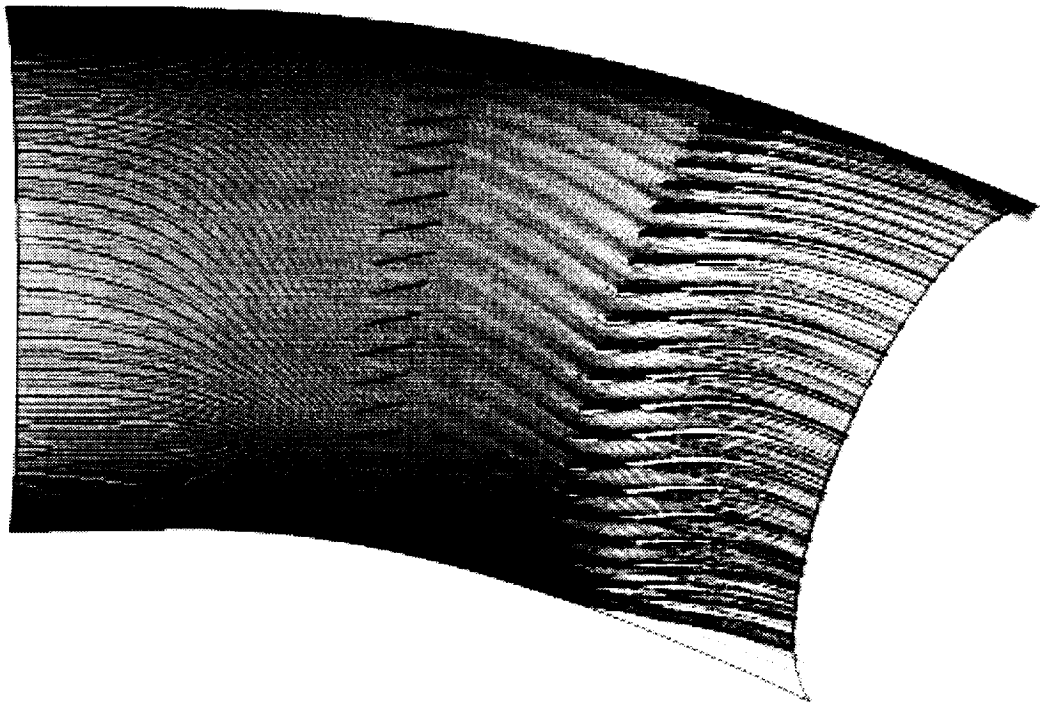

Figure (11): Near wall streamlines within effector region, Maximum Performance "Taguchi Robust" installation design, $\alpha = 0.0^{o}$.

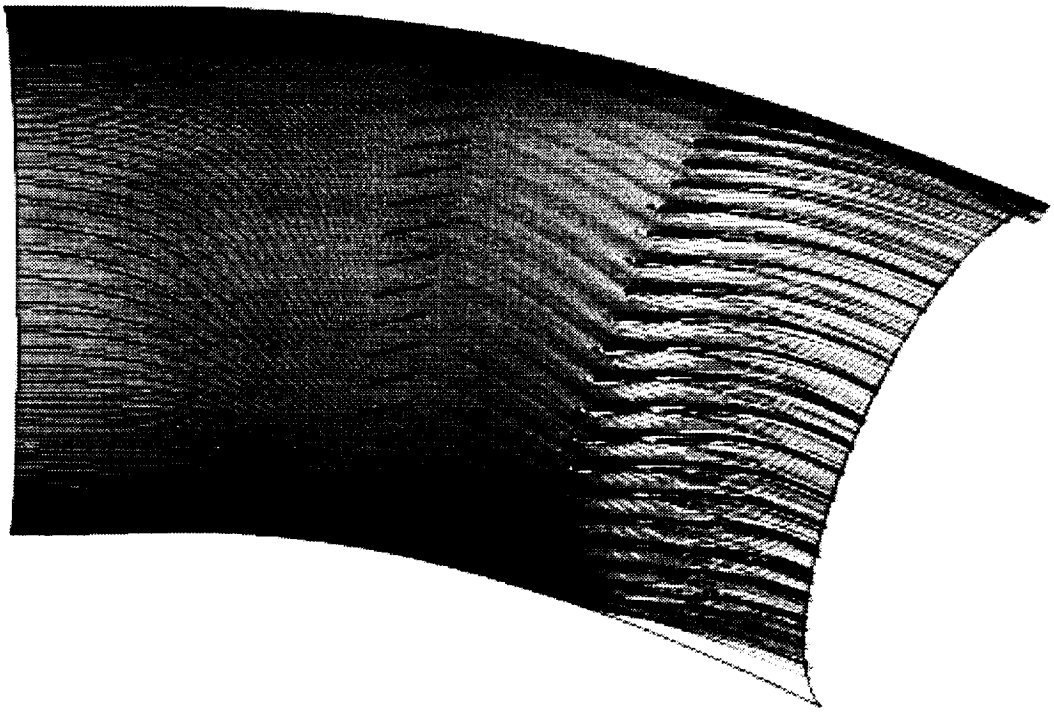

Figure (12): Near wall streamlines within effector region, Maximum Performance "Higher Order Robust" installation design, $\alpha = 0.0^{o}$.

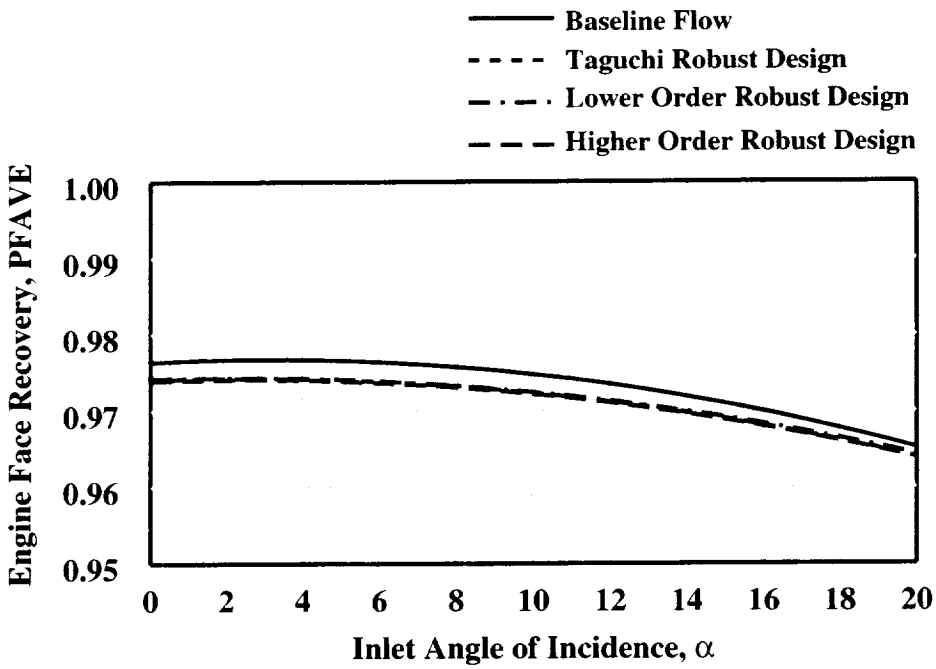

(a) Total Pressure Recovery Characteristics.

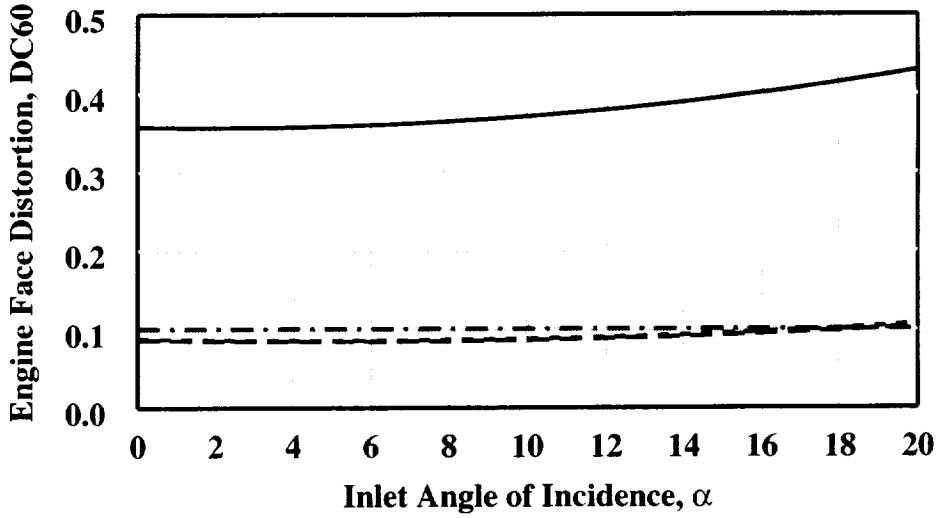

(b) Engine Face DC60 Distortion Characteristics.

Figure (13): Effect of Robust Design methodology on inlet angle-of-incidence performance, Maximum Performance mission.

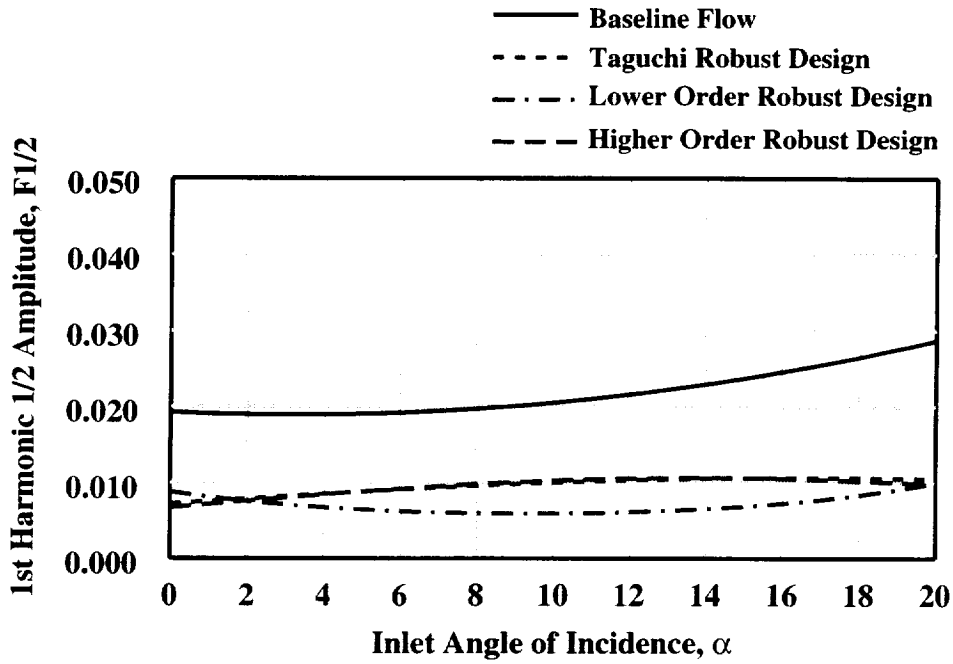

(c) 1st Fourier Harmonic 1/2 Amplitude Characteristics.

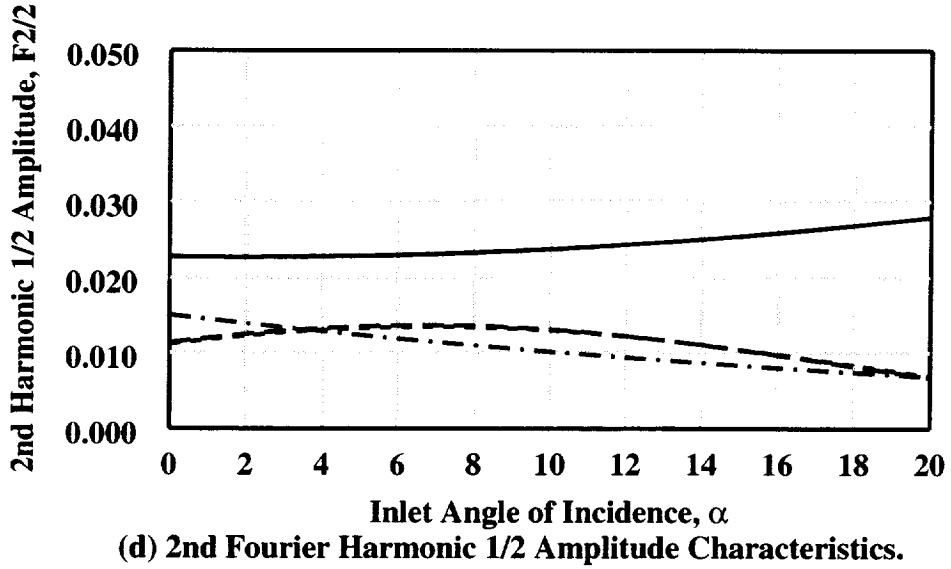

(d) 2nd Fourier Harmonic 1/2 Amplitude Characteristics.

Figure (13): Effect of Robust Design methodology on inlet angle-of-incidence performance, Maximum Performance mission.

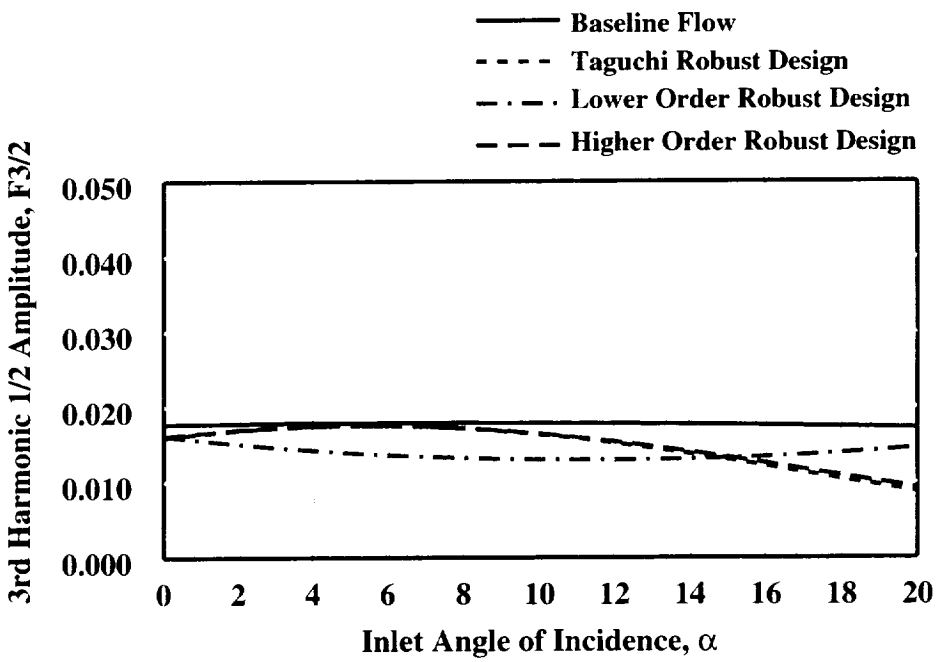

(e) 3rd Fourier Harmonic 1/2 Amplitude Characteristics.

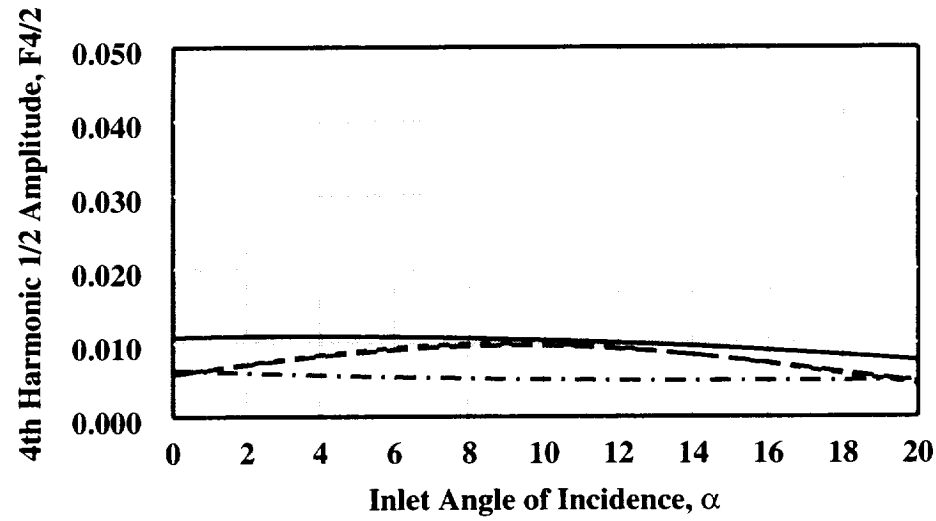

(f) 4th Fourier Harmonic 1/2 Amplitude Characteristics.

Figure (13): Effect of Robust Design methodology on inlet angle-of-incidence performance, Maximum Performance mission.

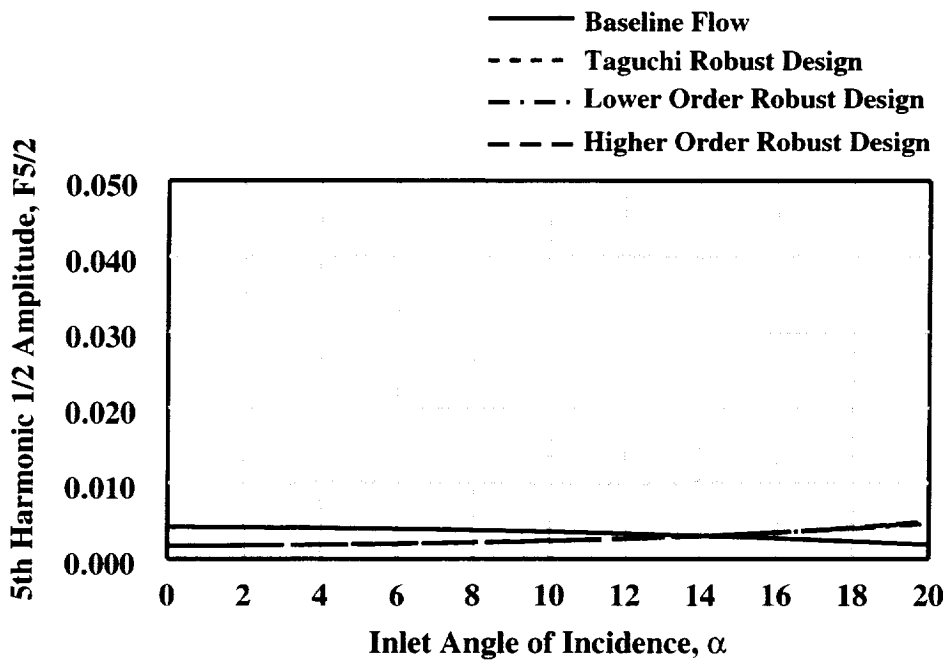

(g) 5th Fourier Harmonic 1/2 Amplitude Characteristics.

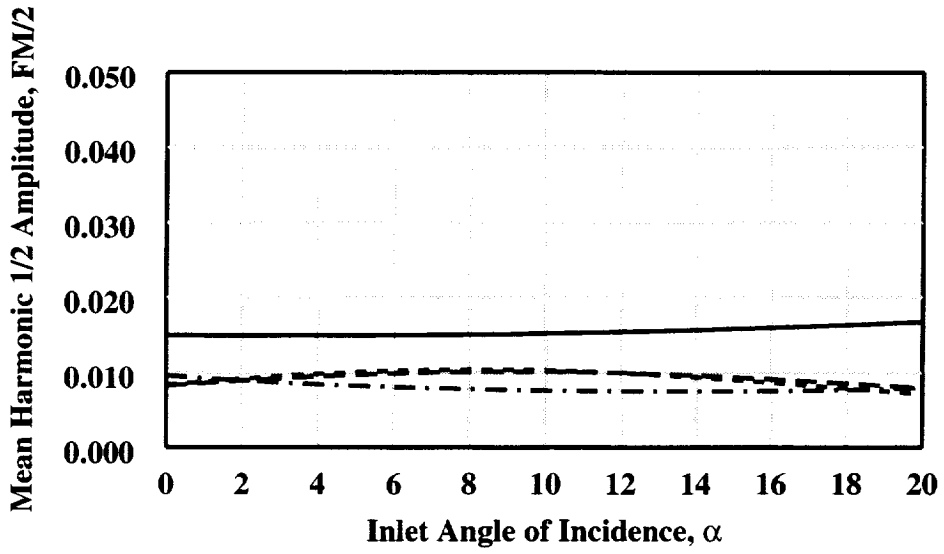

(f) Mean Fourier Harmonic 1/2 Amplitude Characteristics.

Figure (13): Effect of Robust Design methodology on inlet angle-of-incidence performance, Maximum Performance mission.

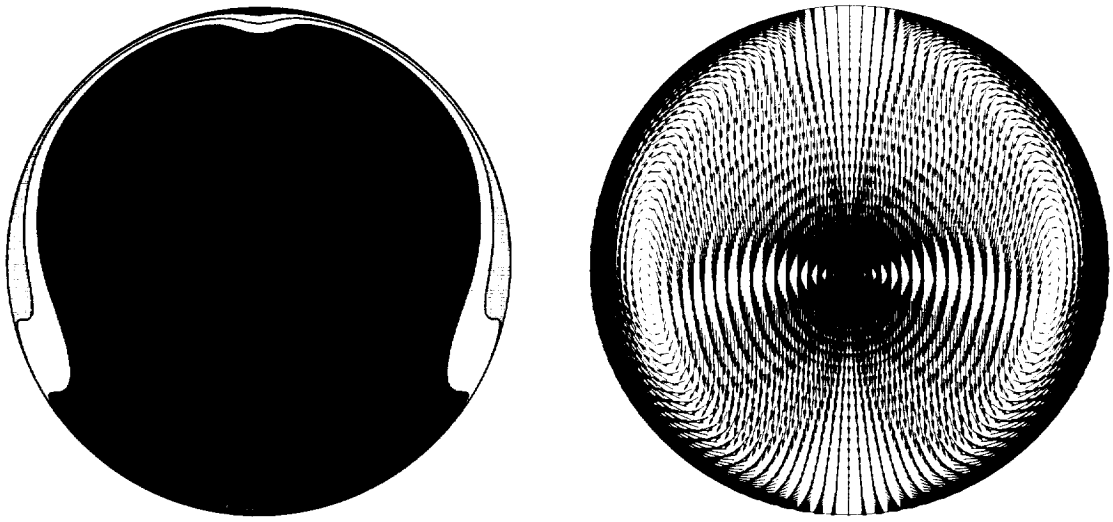

(a) Total pressure recovery contours (b) Secondary flow velocity vectors

Figure (14): Maximum HCF Life Expectancy "Lower Order Robust" installation engine face CFD solution, $\alpha = 0.0^{o}$.

Factor/Response	Range/Constraint	Optimal Value
h_1	0.0 to 2.0	0.0
h_2	0.0 to 2.0	0.0
h_3	0.0 to 2.0	2.00
PFAVE	Unconstrained	0.97377
DC60	≤ 0.10	0.08216
F1/2	Minimized	0.00708
F2/2	Minimized	0.01517
F3/2	Minimized	0.01583
F4/2	Minimized	0.00523
F5/2	Minimized	0.00102
FM/2	Minimized	0.00887

Table (11): Maximum HCF Life Expectancy "Lower Order Robust" installation inlet CFD performance, $\alpha = 0.0^{o}$.

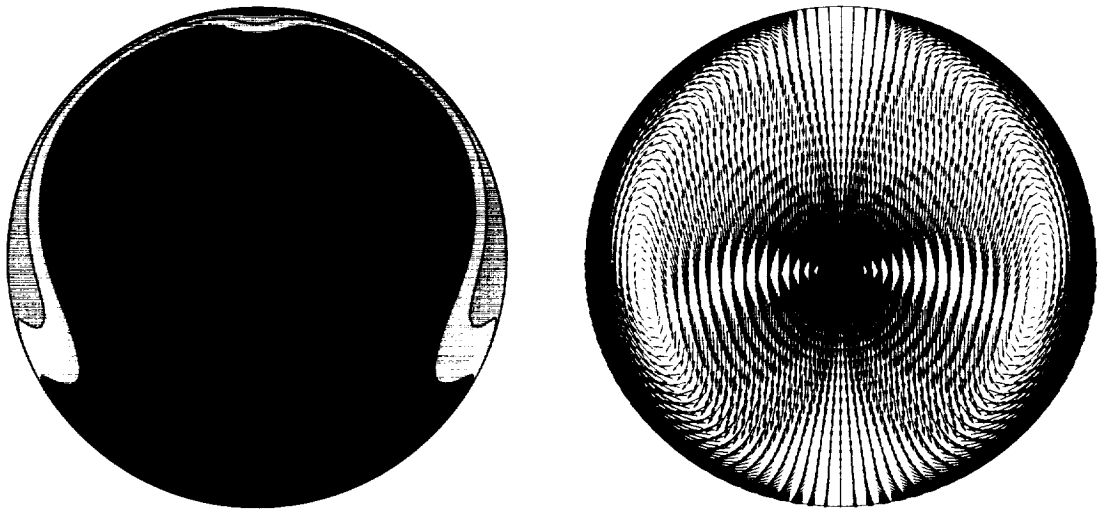

(a) Total pressure recovery contours (b) Secondary flow velocity vectors

Figure (15): Maximum HCF Life Expectancy "Taguchi Robust" installation engine face CFD solution, $\alpha = 0.0^{o}$.

Factor/Response	Range/Constraint	Optimal Value
h_1	0.0 to 2.0	0.0
h_2	0.0 to 2.0	0.52
h_3	0.0 to 2.0	2.00
PFAVE	Unconstrained	0.97274
DC60	≤ 0.10	0.09337
F1/2	Minimized	0.00745
F2/2	Minimized	0.01644
F3/2	Minimized	0.01539
F4/2	Minimized	0.00528
F5/2	Minimized	0.00099
FM/2	Minimized	0.00911

Table (12): Maximum HCF Life Expectancy "Taguchi Robust" installation in inlet CFD performance, $\alpha = 0.0^{o}$.

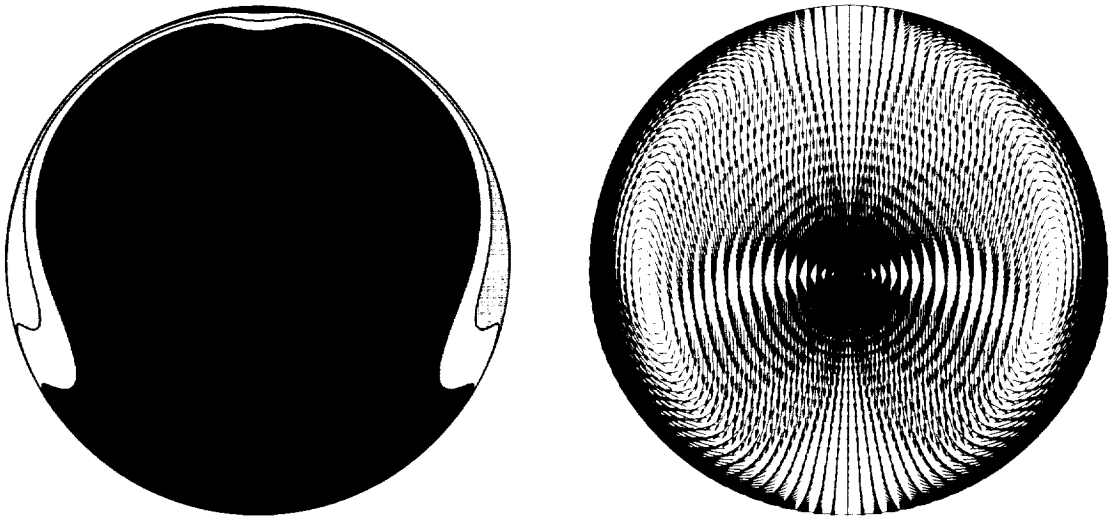

(a) Total pressure recovery contours (b) Secondary flow velocity vectors

Figure (16): Maximum HCF Life Expectancy "Higher Order Robust" installation engine face CFD solution, $\alpha = 0.0^{o}$.

Factor/Response	Range/Constraint	Optimal Value
h_1	0.0 to 2.0	0.0
h_2	0.0 to 2.0	0.40
h_3	0.0 to 2.0	1.90
PFAVE	Unconstrained	0.97315
DC60	≤ 0.10	0.08816
F1/2	Minimized	0.00749
F2/2	Minimized	0.01620
F3/2	Minimized	0.01611
F4/2	Minimized	0.00630
F5/2	Minimized	0.00790
FM/2	Minimized	0.00938

Table (13): Maximum HCF Life Expectancy "Higher Order Robust" installation inlet CFD performance, $\alpha = 0.0^{o}$.

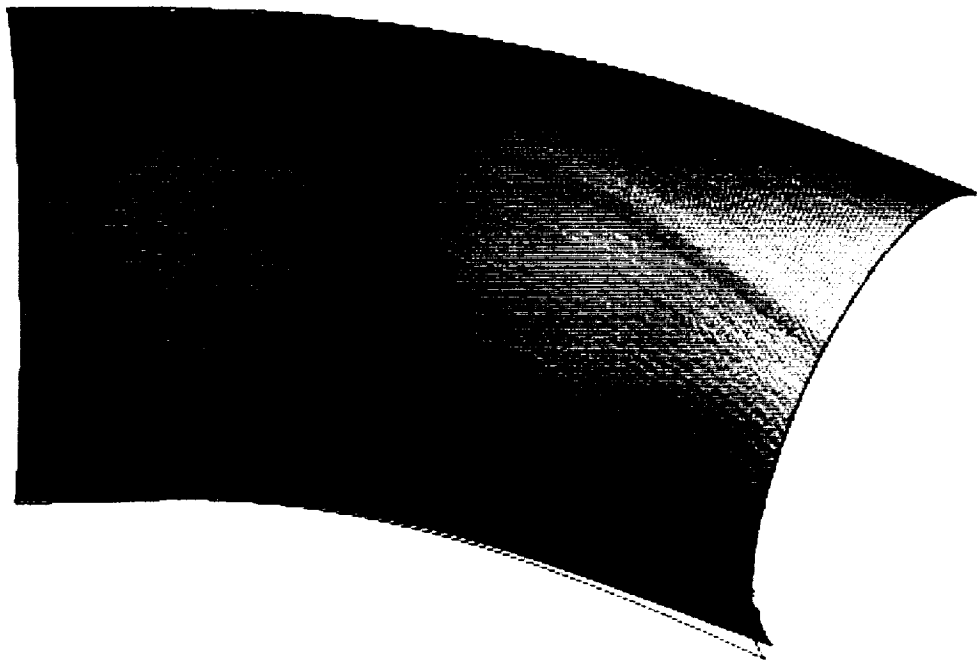

Figure (17): Near wall streamlines, baseline CFD solution, $\alpha = 0.0^{o}$.

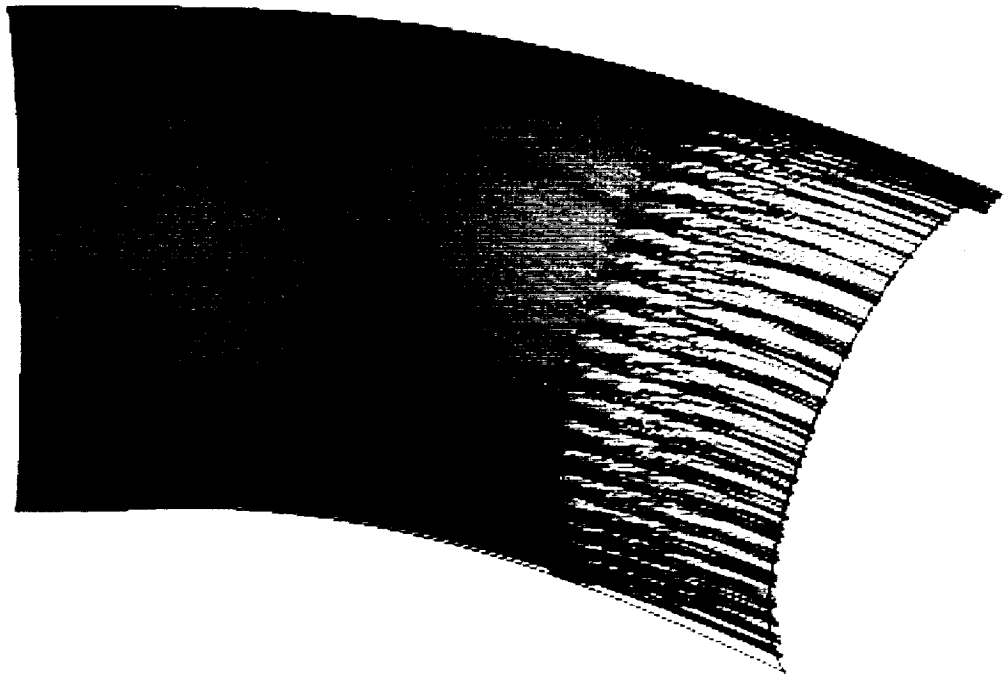

Figure (18): Near wall streamlines, Maximum HCF Life Expectancy "Lower Order Robust" installation design, $\alpha = 0.0^{o}$.

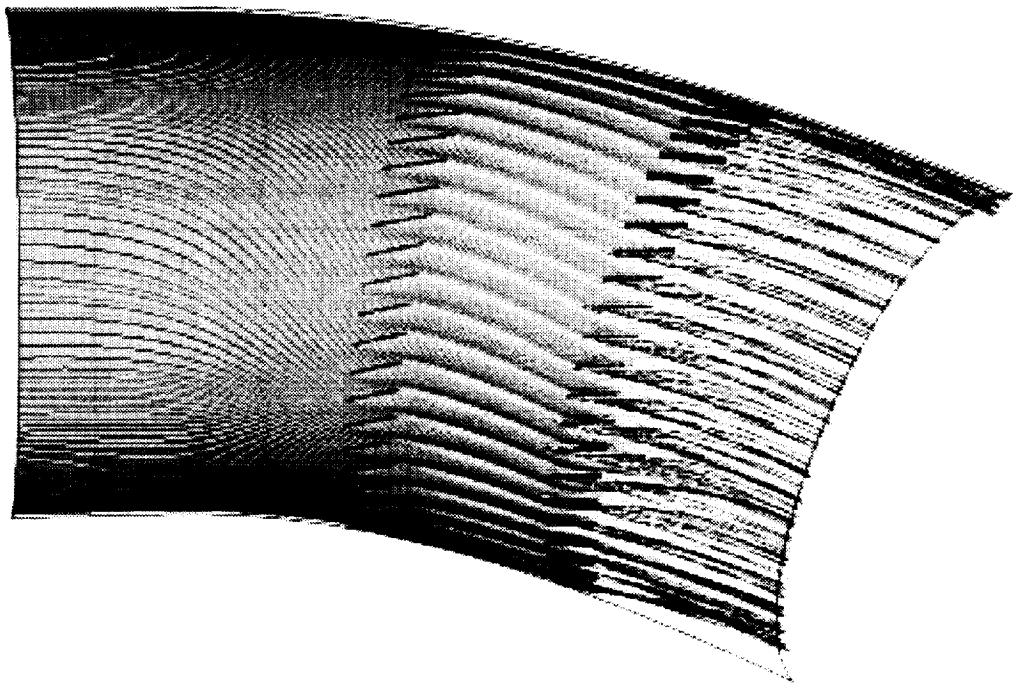

Figure (19): Near wall streamlines, Maximum HCF Life Expectancy "Taguchi Robust" installation design, $\alpha = 0.0^{o}$.

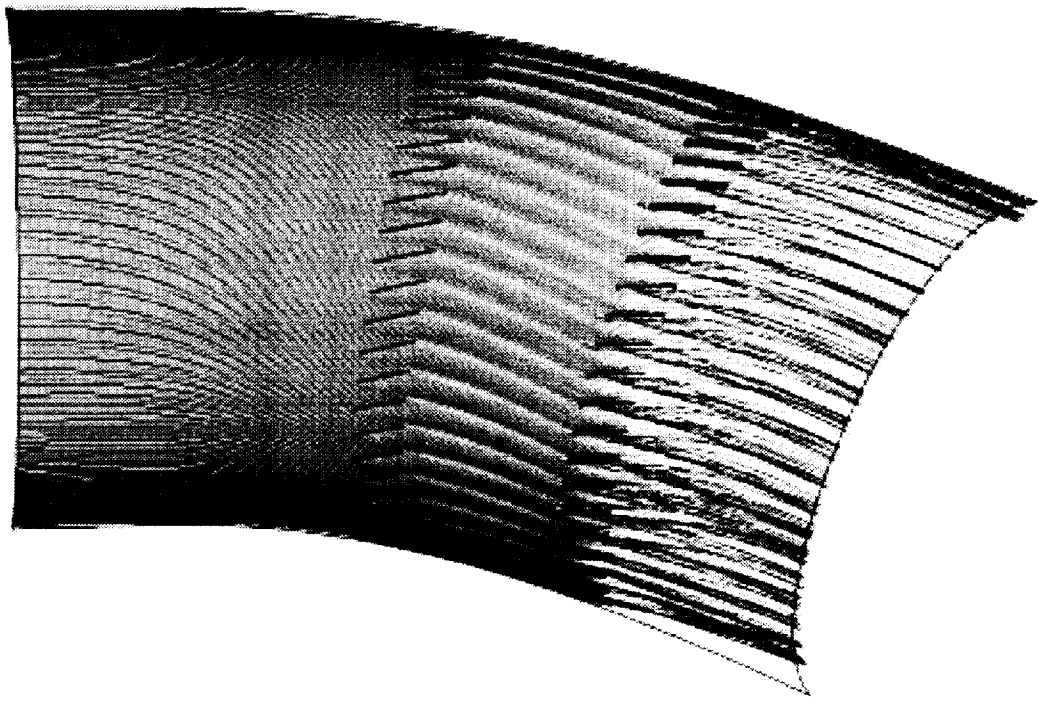

Figure (20): Near wall streamlines, Maximum HCF Life Expectancy "Higher Order Robust" installation design, $\alpha = 0.0^{o}$.

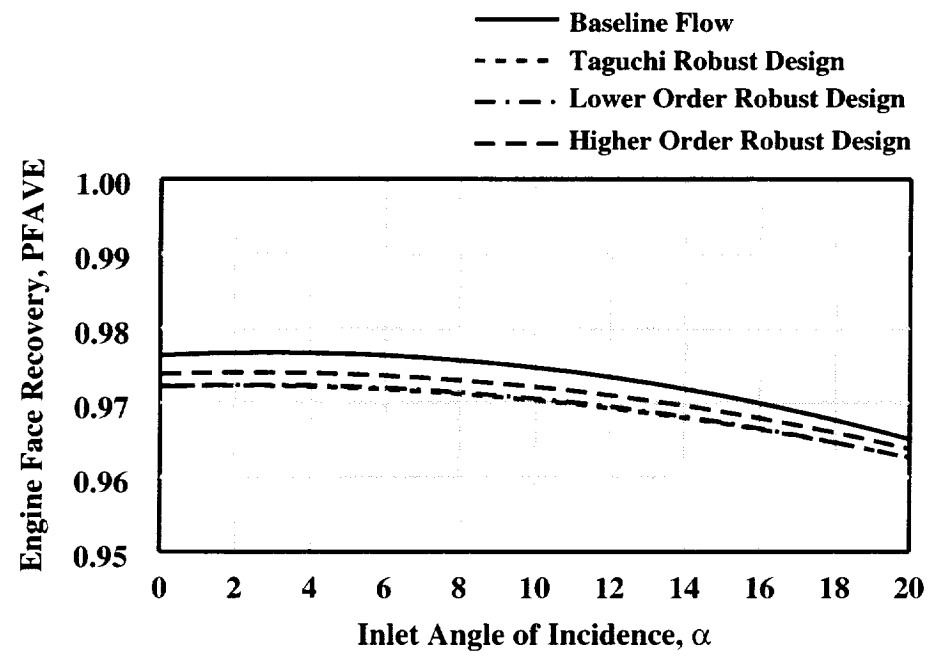

(a) Total Pressure Recovery Characteristics.

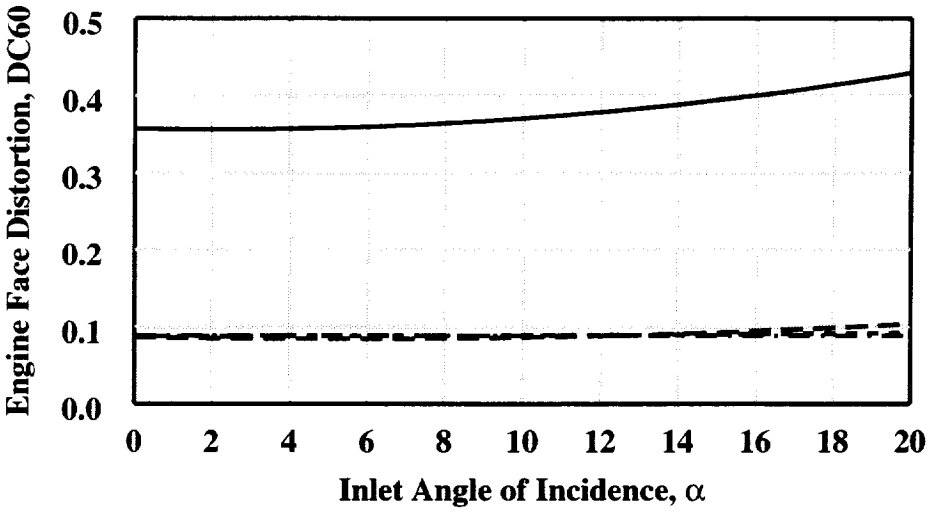

(b) Engine Face DC60 Distortion Characteristics.

Figure (21): Effect of Robust Design methodology on inlet angle-of-incidence performance, Maximum HCF Life Expectancy mission.

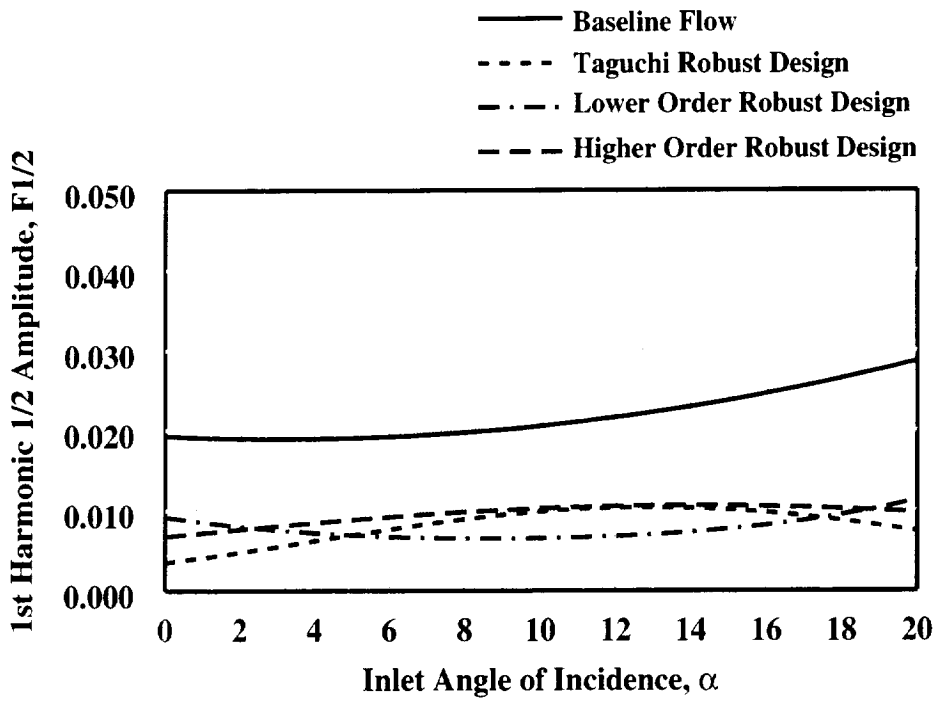

(c) 1st Fourier Harmonic 1/2 Amplitude Characteristics.

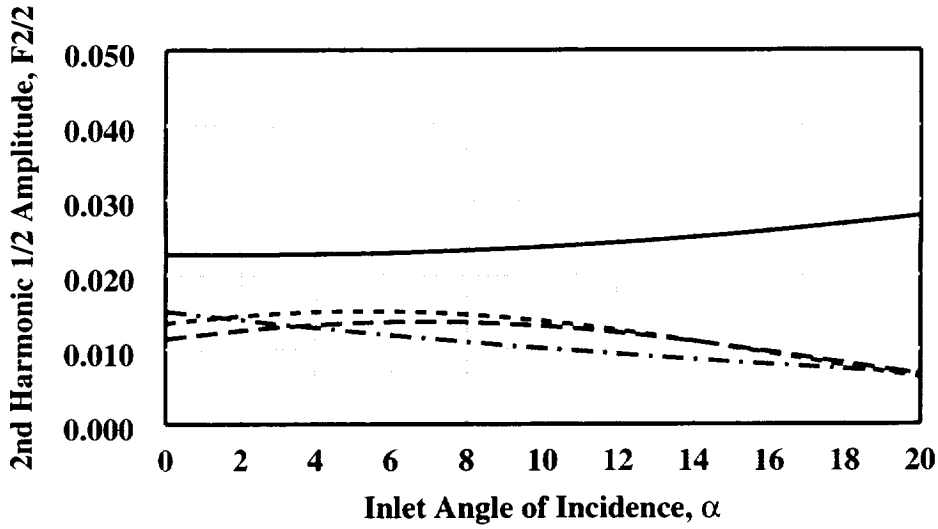

(d) 2nd Fourier Harmonic 1/2 Amplitude Characteristics.

Figure (21): Effect of Robust Design methodology on inlet angle-of-incidence performance, Maximum HCF Life Expectancy mission.

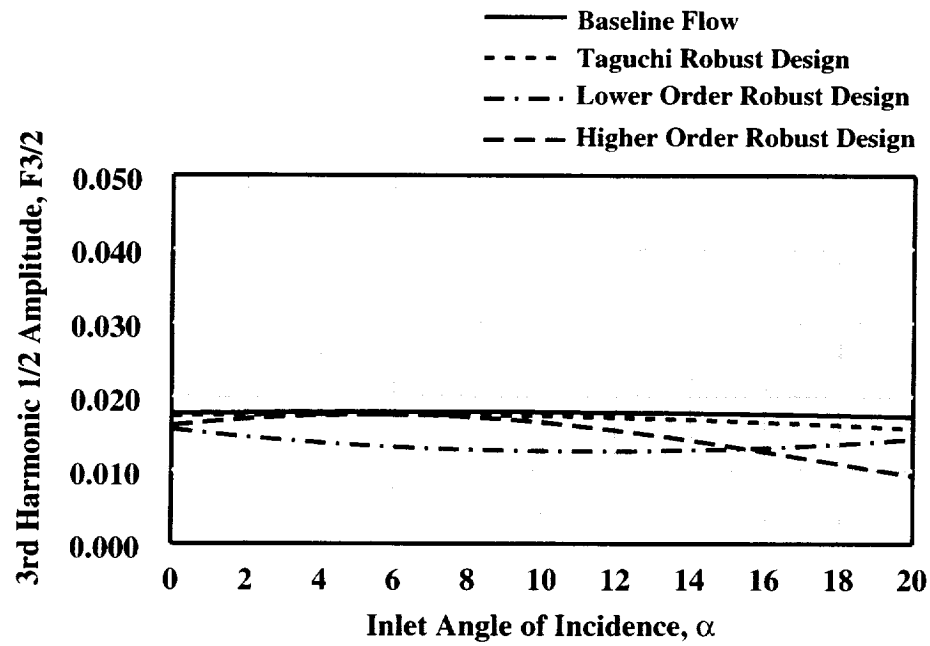

(c) 3rd Fourier Harmonic 1/2 Amplitude Characteristics.

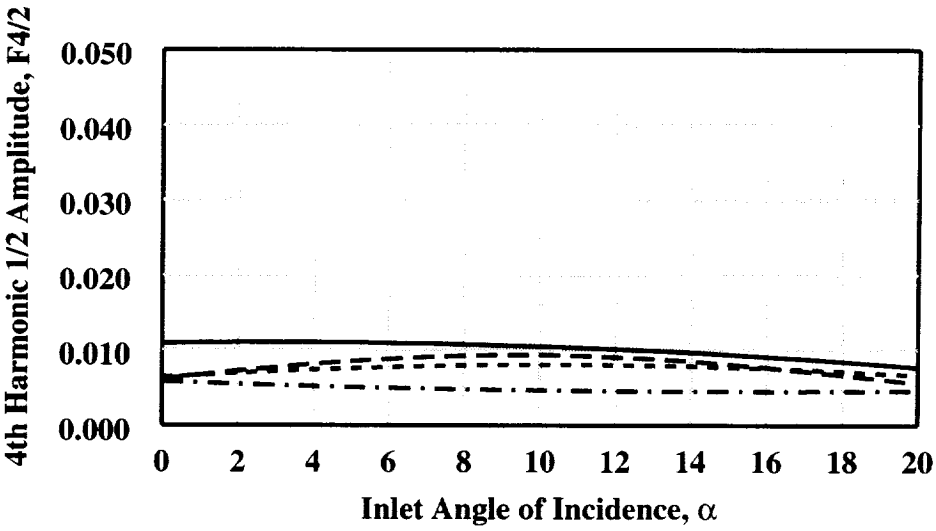

(d) 4th Fourier Harmonic 1/2 Amplitude Characteristics.

Figure (21): Effect of Robust Design methodology on inlet angle-of-incidence performance, Maximum HCF Life Expectancy mission.

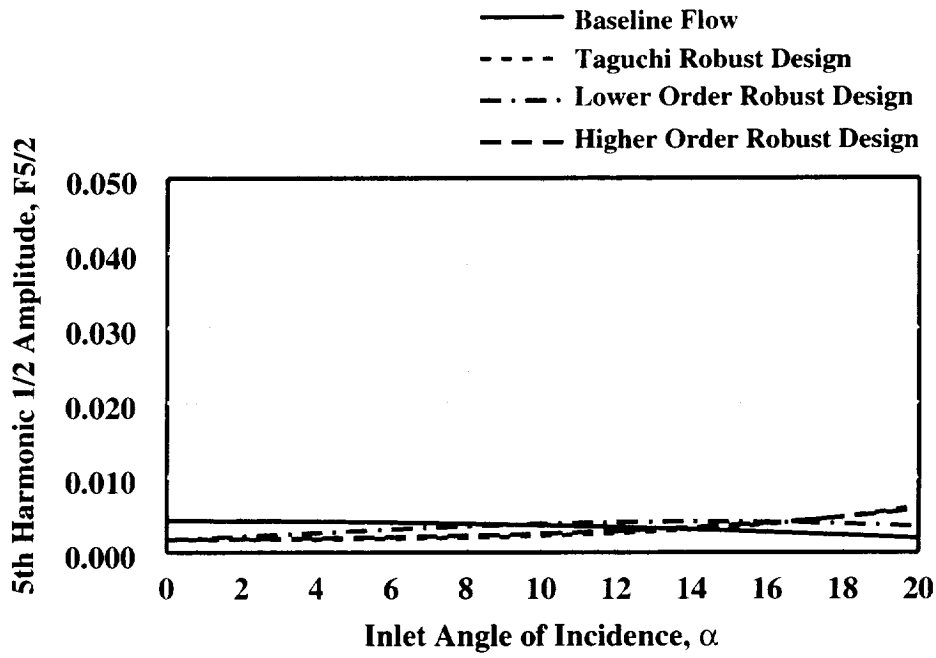

(g) 5th Fourier Harmonic 1/2 Amplitude Characteristics.

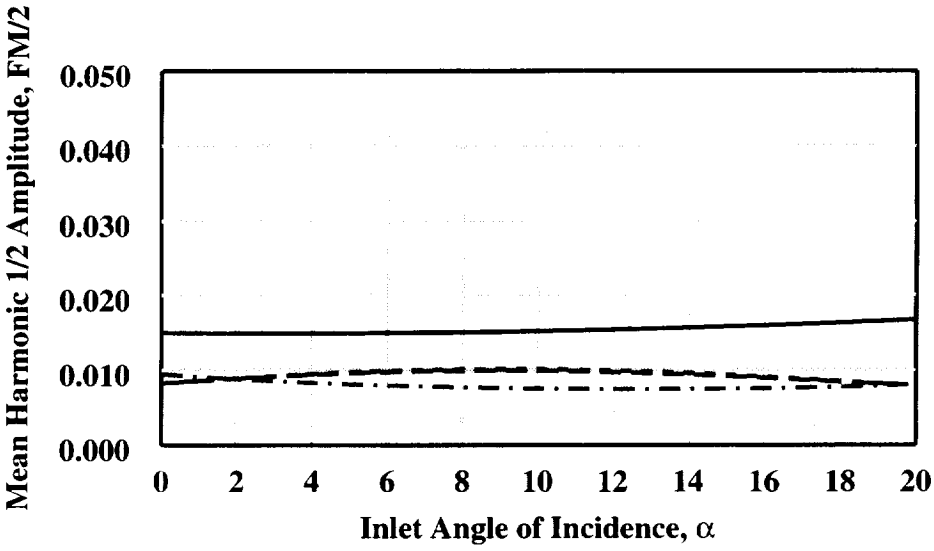

(h) Mean Fourier Harmonic 1/2 Amplitude Characteristics.

Figure (21): Effect of Robust Design methodology on inlet angle-of-incidence performance, Maximum HCF Life Expectancy mission.

Config.	Mission	Optimal Robust	h_1	h_2	h_3	α
nvg555	Max. Performance	Lower Order	0.0	0.0	1.90	0.0
nvg556		Taguchi	0.0	0.06	1.96	
nvg557		Higher Order	0.0	0.05	1.90	
nvg558	Max. HCF Life Exp.	Lower Order	0.0	0.0	2.00	
nvg559		Taguchi	0.0	0.52	2.00	
nvg560		Higher Order	0.0	0.40	1.90	
nvg561	Max. Performance	Lower Order	0.0	0.0	1.90	10.0
nvg562		Taguchi	0.0	0.06	1.96	
nvg563		Higher Order	0.0	0.05	1.90	
nvg564	Max. HCF Life Exp.	Lower Order	0.0	0.0	2.00	
nvg565		Taguchi	0.0	0.52	2.00	
nvg566		Higher Order	0.0	0.40	1.90	
nvg567	Max. Performance	Lower Order	0.0	0.0	1.90	20.0
nvg568		Taguchi	0.0	0.06	1.96	
nvg569		Higher Order	0.0	0.05	1.90	
nvg570	Max. HCF Life Exp.	Lower Order	0.0	0.0	2.00	
nvg571		Taguchi	0.0	0.52	2.00	
nvg572		Higher Order	0.0	0.40	1.90	

Table (14): Optimal MSFC installation CFD validation cases.

Config.	PFAVE	DC60	F1/2	F2/2	F3/2	F4/2	F5/2
nvg555	0.97329	0.08401	0.00705	0.01636	0.01651	0.00527	0.00106
nvg556	0.97379	0.08582	0.00868	0.01757	0.01564	0.00498	0.00077
nvg557	0.97398	0.08570	0.00740	0.01688	0.01634	0.00520	0.00078
nvg558	0.97377	0.08216	0.00708	0.01517	0.01583	0.00523	0.00102
nvg559	0.97274	0.09337	0.00745	0.01644	0.01539	0.00528	0.00099
nvg560	0.97315	0.08816	0.00749	0.01620	0.01611	0.00630	0.00079
nvg561	0.97168	0.08731	0.00450	0.01519	0.01795	0.00435	0.00177
nvg562	0.97183	0.08812	0.00618	0.01650	0.01724	0.00928	0.00117
nvg563	0.97222	0.08825	0.00495	0.01579	0.01772	0.00910	0.00134
nvg564	0.97215	0.08155	0.00590	0.01495	0.01691	0.00471	0.00194
nvg565	0.97112	0.09240	0.00643	0.01722	0.01851	0.00859	0.00166
nvg566	0.97159	0.09105	0.00500	0.01630	0.01854	0.00932	0.00155
nvg567	0.96344	0.09187	0.00828	0.00650	0.01687	0.00547	0.00454
nvg568	0.96378	0.08755	0.00600	0.00886	0.01696	0.00436	0.00377
nvg569	0.96368	0.09087	0.00757	0.00743	0.01688	0.00526	0.00406
nvg570	0.96449	0.08342	0.00681	0.00643	0.01585	0.00450	0.00462
nvg571	0.96312	0.09411	0.00577	0.00952	0.01867	0.00547	0.00506
nvg572	0.96354	0.09388	0.00728	0.00775	0.01777	0.00575	0.00475

Table (15): Optimal MSFC installation CFD validation inlet performance results.

Factor	α	LOG(Y_{DOE})	LOG(Y_{CFD})	t	t*	Comment
PFAVE	0.0	0.974175	0.973290	2.119905	2.117512	Not Diff.
DC60		-2.292872	-2.476819	2.093024	0.851971	Not Diff.
F1/2		-4.731187	-4.9554728	1.969576	0.462868	Not Diff.
F2/2		-4.195049	-4.112916	1.969460	0.168647	Not Diff.
F3/2		-4.125588	-4.103789	1.969654	0.266407	Not Diff.
F4/2		-5.061823	-5.245725	1.969498	0.892816	Not Diff.
F5/2		-6.365431	-6.849486	1.969422	1.157973	Not Diff.
PFAVE	10.0	0.972422	0.971680	2.119905	1.820567	Not Diff.
DC60		-2.292872	-2.438290	2.093024	0.673197	Not Diff.
F1/2		-5.117998	-5.403678	1.969576	0.635825	Not Diff.
F2/2		-4.195049	-4.187118	1.969460	0.016286	Not Diff.
F3/2		-4.169370	-4.342960	1.969654	3.662619	Diff.
F4/2		-5.286389	-5.437579	1.969498	0.779770	Not Diff.
F5/2		-5.568553	-6.336776	1.969422	1.912303	Not Diff.
PFAVE	20.0	0.964306	0.963440	2.119905	2.072052	Not Diff.
DC60		-2.292872	-2.387381	2.093024	0.4377726	Not Diff.
F1/2		-4.609279	-4.793912	1.969576	0.421698	Not Diff.
F2/2		-4.195049	-5.035953	1.969460	1.726653	Not Diff.
F3/2		-4.226871	-4.082218	1.969654	1.641479	Not Diff.
F4/2		-5.061823	-5.108477	1.969498	0.711981	Not Diff.
F5/2		-5.683392	-5.394828	1.969422	0.691661	Not Diff.

Table (16): Comparison of DOE predicted and CFD analysis inlet performance, "Lower Order" Robust Design methodology, optimal Maximum Performance installation, $h_1 = 0.0$, $h_2 = 0.0$, $h_3 = 1.9$.

Factor	α	LOG(Y_{DOE})	LOG(Y_{CFD})	t	t*	Comment
PFAVE	0.0	0.974031	0.973790	2.032245	0.973700	Not Diff.
DC60		-2.427128	-2.455503	2.015368	0.129396	Not Diff.
F1/2		-4.105304	-4.746734	1.964581	0.456548	Not Diff.
F2/2		-4.492556	-4.041562	1.964519	0.828663	Not Diff.
F3/2		-4.134229	-4.157924	1.964545	0.250316	Not Diff.
F4/2		-5.153179	-5.320563	1.964545	1.434832	Not Diff.
F5/2		-6.346997	-7.169120	1.964484	1.784047	Not Diff.
PFAVE	10.0	0.972310	0.971830	2.032245	1.990771	Not Diff.
DC60		-2.427321	-2.429056	2.015368	0.008423	Not Diff.
F1/2		-4.606671	-5.086437	1.964581	1.414476	Not Diff.
F2/2		-4.346505	-4.104395	1.964519	0.442960	Not Diff.
F3/2		-4.110596	-4.060523	1.964545	0.508612	Not Diff.
F4/2		-4.621910	-4.679894	1.964545	0.692970	Not Diff.
F5/2		-6.027714	-6.750752	1.964484	1.629661	Not Diff.
PFAVE	20.0	0.963921	0.963780	2.032245	0.569675	Not Diff.
DC60		-2.233236	-2.435545	2.015368	0.922583	Not Diff.
F1/2		-4.556761	-5.115996	1.964581	1.660996	Not Diff.
F2/2		-4.977829	-4.726209	1.964519	0.466095	Not Diff.
F3/2		-4.730847	-4.076869	1.964545	6.458209	Diff.
F4/2		-5.407909	-5.435283	1.964545	0.336713	Not Diff.
F5/2		-5.323840	-5.580680	1.964484	0.566588	Not Diff.

Table (17): Comparison of DOE predicted and CFD analysis inlet performance, "Taguchi" Robust Design methodology, optimal Maximum Performance installation, $h_1 = 0.0$, $h_2 = 0.06$, $h_3 = 1.96$.

Factor	α	LOG(Y_{DOE})	LOG(Y_{CFD})	t	t*	Comment
PFAVE	0.0	0.974141	0.973980	2.032245	0.657011	Not Diff.
DC60		-2.400661	-2.456902	2.015368	0.257866	Not Diff.
F1/2		-4.936734	-4.906275	1.964581	0.074077	Not Diff.
F2/2		-4.517984	-4.081626	1.964519	0.804010	Not Diff.
F3/2		-4.126826	-4.114139	1.964545	0.133861	Not Diff.
F4/2		-5.137049	-5.259097	1.964545	1.084938	Not Diff.
F5/2		-6.361949	-7.156217	1.964484	1.737920	Not Diff.
PFAVE	10.0	0.972407	0.972220	2.032245	0.780349	Not Diff.
DC60		-2.397357	-2.427582	2.015368	0.147374	Not Diff.
F1/2		-4.658782	-5.308368	1.964581	1.928640	Not Diff.
F2/2		-5.450769	-4.148378	1.964519	1.194816	Not Diff.
F3/2		-4.109194	-4.033061	1.964545	0.772896	Not Diff.
F4/2		-4.600481	-4.699481	1.964545	1.198590	Not Diff.
F5/2		6.003537	6.615086	1.964484	1.385402	Not Diff.
PFAVE	20.0	0.963971	0.964380	2.032245	1.189906	Not Diff.
DC60		-2.197703	-2.398325	2.015368	0.919857	Not Diff.
F1/2		-4.450305	-4.883562	1.964581	1.289536	Not Diff.
F2/2		-4.969445	-4.902229	1.964519	0.124723	Not Diff.
F3/2		-4.759488	-4.081626	1.964545	6.760066	Diff.
F4/2		-5.447282	-5.247624	1.964545	2.622528	Diff.
F5/2		-5.326100	-5.506572	1.964484	0.399723	Not Diff.

Table (18): Comparison of DOE predicted and CFD analysis inlet performance, "Higher Order" Robust Design methodology, optimal Maximum Performance installation, $h_1 = 0.0$, $h_2 = 0.05$, $h_3 = 1.90$.

Factor	α	LOG(Y_{DOE})	LOG(Y_{CFD})	t	t*	Comment
PFAVE	0.0	0.974070	0.973770	2.119905	0.711378	Not Diff.
DC60		-2.354837	-2.354837	2.093024	0.659571	Not Diff.
F1/2		-4.688334	-4.843427	1.969576	0.314626	Not Diff.
F2/2		-4.195049	-4.124598	1.969460	0.144660	Not Diff.
F3/2		-4.162474	-4.145848	1.969654	0.203505	Not Diff.
F4/2		-5.148175	-5.215816	1.969498	0.326621	Not Diff.
F5/2		-6.394333	-6.489045	1.969422	0.225952	Not Diff.
PFAVE	10.0	0.972330	0.972150	2.119905	0.439612	Not Diff.
DC60		-2.354837	-2.506539	2.093024	0.693646	Not Diff.
F1/2		-5.032574	-5.132803	1.969576	0.219701	Not Diff.
F2/2		-4.589592	-4.203044	1.969460	0.811770	Not Diff.
F3/2		-4.372424	-4.079850	1.969654	3.309550	Diff.
F4/2		-5.372825	-5.358067	1.969498	0.075280	Not Diff.
F5/2		-5.568553	-6.245067	1.969422	1.684017	Not Diff.
PFAVE	20.0	0.964227	0.964490	2.119905	0.623641	Not Diff.
DC60		-2.354837	-2.483867	2.093024	0.589981	Not Diff.
F1/2		-4.481273	-4.989363	1.969576	1.150719	Not Diff.
F2/2		-4.984091	-5.046781	1.969460	0.130797	Not Diff.
F3/2		-4.250998	-4.114586	1.969654	1.205920	Not Diff.
F4/2		-5.383004	-5.403678	1.969498	0.104769	Not Diff.
F5/2		-5.564421	-5.377361	1.969422	0.662514	Not Diff.

Table (19): Comparison of DOE predicted and CFD analysis inlet performance, "Lower Order" Robust Design methodology, optimal Maximum HCF Life Expectancy installation, $h_1 = 0.0$, $h_2 = 0.0$, $h_3 = 2.0$.

Factor	α	LOG(Y_{DOE})	LOG(Y_{CFD})	t	t*	Comment
PFAVE	0.0	0.973041	0.972740	2.032245	1.253495	Not Diff.
DC60		-2.435739	-2.371185	2.015368	0.304126	Not Diff.
F1/2		-5.497500	-4.773589	1.964581	1.698227	Not Diff.
F2/2		-4.427191	-3.993233	1.964519	0.792779	Not Diff.
F3/2		-4.046183	-4.051860	1.964545	0.057842	Not Diff.
F4/2		-5.103903	-5.170804	1.964545	0.773349	Not Diff.
F5/2		-6.349855	-6.917086	1.964484	1.222402	Not Diff.
PFAVE	10.0	0.971254	0.971120	2.032245	0.566156	Not Diff.
DC60		-2.433009	-2.381628	2.015368	0.238496	Not Diff.
F1/2		-4.646305	-5.046781	1.964581	1.219150	Not Diff.
F2/2		-5.123860	-4.061684	1.964519	1.956620	Not Diff.
F3/2		-4.058148	-3.989444	1.964545	0.698267	Not Diff.
F4/2		-4.741563	-4.757157	1.964545	0.224227	Not Diff.
F5/2		-6.040235	-6.400938	1.964484	0.816500	Not Diff.
PFAVE	20.0	0.963236	0.963120	2.032245	0.483075	Not Diff.
DC60		-2.235046	-2.363291	2.015368	0.180179	Not Diff.
F1/2		-4.712421	-5.155083	1.964581	1.345302	Not Diff.
F2/2		-5.123860	-4.654360	1.964519	0.864859	Not Diff.
F3/2		-4.364658	3.980837	1.964545	3.799567	Diff.
F4/2		-5.085143	-5.208477	1.964545	1.329526	Not Diff.
F5/2		-5.123356	-5.286389	1.964484	0.357475	Not Diff.

Table (20): Comparison of DOE predicted and CFD analysis inlet performance, "Taguchi" Robust Design methodology, optimal Maximum HCF Life Expectancy installation, $h_1 = 0.0$, $h_2 = 0.52$, $h_3 = 2.0$.

Factor	α	LOG(Y_{DOE})	LOG(Y_{CFD})	t	t*	Comment
PFAVE	0.0	0.973435	0.973150	2.032245	1.204137	Not Diff.
DC60		-2.399085	-2.428602	2.015368	0.139424	Not Diff.
F1/2		-5.418904	-4.894186	1.964581	1.307836	Not Diff.
F2/2		-4.489256	4.062846	1.964519	0.784385	Not Diff.
F3/2		-4.038721	-4.068092	1.964545	0.304142	Not Diff.
F4/2		-5.093419	-5.067206	1.964545	0.306455	Not Diff.
F5/2		-6.370093	-7.143478	1.964484	1.692962	Not Diff.
PFAVE	10.0	0.971747	0.971590	2.032245	0.243357	Not Diff.
DC60		-2.389396	-2.396346	2.015368	0.034372	Not Diff.
F1/2		-5.046314	-5.298317	1.964581	0.572888	Not Diff.
F2/2		-4.413385	-4.116590	1.964519	0.5777779	Not Diff.
F3/2		-4.061800	-3.987825	1.964545	0.756262	Not Diff.
F4/2		-4.683240	-4.675593	1.964545	0.108026	Not Diff.
F5/2		-5.989467	-6.469500	1.964484	1.089642	Not Diff.
PFAVE	20.0	0.963476	0.963540	2.032245	0.270966	Not Diff.
DC60		-4.213128	-2.365738	2.015368	1.561665	Not Diff.
F1/2		-4.521381	-4.922624	1.964581	1.220646	Not Diff.
F2/2		-5.100615	-4.860062	1.964519	0.445740	Not Diff.
F3/2		-4.475898	-4.030244	1.964545	4.470297	Diff.
F4/2		-5.191977	5.158555	1.964545	0.417533	Not Diff.
F5/2		-5.295521	-5.349611	1.964484	0.103381	Not Diff.

Table (21): Comparison of DOE predicted and CFD analysis inlet performance, "Higher Order" Robust Design methodology, optimal Maximum HCF Life Expectancy installation, $h_1 = 0.0$, $h_2 = 0.4$, $h_3 = 1.9$

Factor	α	LOG(Y_{LOR})	LOG(Y_{TR})	t	t*	Comment
PFAVE	0.0	0.974175	0.974031	2.076075	0.296459	Not Diff.
DC60		-2.292872	-2.427128	2.054196	0.436268	Not Diff.
F1/2		-4.731187	-4.105304	1.967079	0.325906	Not Diff.
F2/2		-4.195049	-4.492556	1.966989	0.407359	Not Diff.
F3/2		-4.125588	-4.134229	1.967100	0.069069	Not Diff.
F4/2		-5.061823	-5.153179	1.967021	0.385921	Not Diff.
F5/2		-6.365431	-6.346997	1.966953	0.029628	Not Diff.
PFAVE	10.0	0.972422	0.972310	2.076075	2.336514	Not Diff.
DC60		-2.292872	-2.427321	2.053696	0.450472	Not Diff.
F1/2		-5.117998	-4.606671	1.967079	0.908286	Not Diff.
F2/2		-4.195049	-4.346505	1.966989	0.206887	Not Diff.
F3/2		-4.169370	-4.110596	1.967100	1.758532	Not Diff.
F4/2		-5.286389	-4.621910	1.967021	3.146564	Diff.
F5/2		-5.568553	-6.027714	1.966953	0.767156	Not Diff.
PFAVE	20.0	0.964306	0.963921	2.076075	0.792615	Not Diff.
DC60		-2.292872	-2.233236	2.054196	0.193789	Not Diff.
F1/2		-4.609279	-4.556761	1.967079	0.095086	Not Diff.
F2/2		-4.195049	-4.977829	1.966989	1.076635	Not Diff.
F3/2		-4.226871	-4.730847	1.967100	3.754435	Diff.
F4/2		-5.061823	-5.407909	1.967021	1.562868	Not Diff.
F5/2		-5.683392	-5.323840	1.966953	0.583616	Not Diff.

Table (22): Comparison of "Lower Order" and "Taguchi" Robust Design methodology, optimal Maximum Performance mission.

Factor	α	LOG(Y_{HOR})	LOG(Y_{TR})	t	t*	Comment
PFAVE	0.0	0.974141	0.974031	2.032245	0.315823	Not Diff.
DC60		-2.400661	-2.427128	2.015368	0.085577	Not Diff.
F1/2		-4.936734	-4.105304	1.964581	0.007079	Not Diff.
F2/2		-4.517984	-4.492556	1.964519	0.033083	Not Diff.
F3/2		-4.126826	-4.134229	1.964545	0.055267	Not Diff.
F4/2		-5.137049	-5.153179	1.964545	0.099527	Not Diff.
F5/2		-6.361949	-6.346997	1.964484	0.023037	Not Diff.
PFAVE	10.0	0.972407	0.972310	2.032245	0.285342	Not Diff.
DC60		-2.397357	-2.427321	2.015368	0.103091	Not Diff.
F1/2		-4.658782	-4.606671	1.964581	0.109018	Not Diff.
F2/2		-5.450769	-4.346505	1.964519	0.905586	Not Diff.
F3/2		-4.109194	-4.110596	1.964545	0.010064	Not Diff.
F4/2		-4.600481	-4.621910	1.964545	0.182253	Not Diff.
F5/2		6.003537	-6.027714	1.964484	0.038629	Not Diff.
PFAVE	20.0	0.963971	0.963921	2.032245	0.143699	Not Diff.
DC60		-2.197703	-2.233236	2.015368	0.114891	Not Diff.
F1/2		-4.450305	-4.556761	1.964581	0.223812	Not Diff.
F2/2		-4.969445	-4.977829	1.964519	0.010991	Not Diff.
F3/2		-4.759488	-4.730847	1.964545	0.200978	Not Diff.
F4/2		-5.447282	-5.407909	1.964545	0.353498	Not Diff.
F5/2		-5.326100	-5.323840	1.964484	0.003531	Not Diff.

Table (23): Comparison of "Higher Order" and "Taguchi" Robust Design methodology, optimal Maximum Performance mission.

Factor	α	LOG(Y_{LOR})	LOG(Y_{HOR})	t	t*	Comment
PFAVE	0.0	0.974175	0.974141	2.076075	0.070178	Not Diff.
DC60		-2.292872	-2.400661	2.054196	0.351223	Not Diff.
F1/2		-4.731187	-4.936734	1.967079	0.324066	Not Diff.
F2/2		-4.195049	-4.517984	1.966989	0.442869	Not Diff.
F3/2		-4.125588	-4.126826	1.967100	0.009894	Not Diff.
F4/2		-5.061823	-5.137049	1.967021	0.320525	Not Diff.
F5/2		-6.365431	-6.361949	1.966953	0.005622	Not Diff.
PFAVE	10.0	0.972422	0.972407	2.076075	0.031726	Not Diff.
DC60		-2.292872	-2.397357	2.053696	0.350786	Not Diff.
F1/2		-5.117998	-4.658782	1.967079	0.917792	Not Diff.
F2/2		-4.195049	-5.450769	1.966989	1.051794	Not Diff.
F3/2		-4.169370	-4.109194	1.967100	1.768606	Not Diff.
F4/2		-5.286389	-4.600481	1.967021	3.254583	Diff.
F5/2		-5.568553	6.003537	1.966953	0.728792	Not Diff.
PFAVE	20.0	0.964306	0.963971	2.076075	0.691811	Not Diff.
DC60		-2.292872	-2.197703	2.054196	0.310105	Not Diff.
F1/2		-4.609279	-4.450305	1.967079	0.288054	Not Diff.
F2/2		-4.195049	-4.969445	1.966989	1.066112	Not Diff.
F3/2		-4.226871	-4.759488	1.967100	3.989818	Diff.
F4/2		-5.061823	-5.447282	1.967021	1.755287	Not Diff.
F5/2		-5.683392	-5.326100	1.966953	0.581208	Not Diff.

Table (24): Comparison of "Lower Order" and "Higher Order" Robust Design methodology, optimal Maximum Performance mission.

Factor	α	LOG(Y_{LOR})	LOG(Y_{TR})	t	t*	Comment
PFAVE	0.0	0.974070	0.973041	2.076075	2.120379	Diff.
DC60		-2.354837	-2.435739	2.054196	0.265453	Not Diff.
F1/2		-4.688334	-5.497500	1.967079	1.241636	Not Diff.
F2/2		-4.195049	-4.427191	1.966989	0.316841	Not Diff.
F3/2		-4.162474	-4.046183	1.967100	0.910690	Not Diff.
F4/2		-5.148175	-5.103903	1.967021	0.197259	Not Diff.
F5/2		-6.394333	-6.349855	1.966953	0.071078	Not Diff.
PFAVE	10.0	0.972330	0.971254	2.076075	2.275139	Diff.
DC60		-2.354837	-2.433009	2.053696	0.252004	Not Diff.
F1/2		-5.032574	-4.646305	1.967079	0.687112	Not Diff.
F2/2		-4.589592	-5.123860	1.966989	0.739868	Not Diff.
F3/2		-4.372424	-4.058148	1.967100	2.379903	Diff.
F4/2		-5.372825	-4.741563	1.967021	3.034837	Diff.
F5/2		-5.568553	-6.040235	1.966953	0.789939	Not Diff.
PFAVE	20.0	0.964227	0.963236	2.076075	2.042075	Not Diff.
DC60		-2.354837	-2.235046	2.054196	0.097747	Not Diff.
F1/2		-4.481273	-4.712421	1.967079	0.419766	Not Diff.
F2/2		-4.984091	-5.123860	1.966989	0.193006	Not Diff.
F3/2		-4.250998	-4.364658	1.967100	0.847382	Not Diff.
F4/2		-5.383004	-5.085143	1.967021	1.366055	Not Diff.
F5/2		-5.564421	-5.123356	1.966953	0.858249	Not Diff.

Table (25): Comparison of "Lower Order" and "Taguchi" Robust Design methodology, optimal Maximum HCF Life Expectancy mission.

Factor	α	LOG(Y_{HOR})	LOG(Y_{TR})	t	t*	Comment
PFAVE	0.0	0.973435	0.973041	2.032245	1.168563	Not Diff.
DC60		-2.399085	-2.435739	2.015368	0.122267	Not Diff.
F1/2		-5.418904	-5.497500	1.964581	0.134263	Not Diff.
F2/2		-4.489256	-4.427191	1.964519	0.080450	Not Diff.
F3/2		-4.038721	-4.046183	1.964545	0.054198	Not Diff.
F4/2		-5.093419	-5.103903	1.964545	0.086171	Not Diff.
F5/2		-6.370093	-6.349855	1.964484	0.031059	Not Diff.
PFAVE	10.0	0.971747	0.971254	2.032245	1.180228	Not Diff.
DC60		-2.389396	-2.433009	2.015368	0.141796	Not Diff.
F1/2		-5.046314	-4.646305	1.964581	0.690292	Not Diff.
F2/2		-4.413385	-5.123860	1.964519	0.900347	Not Diff.
F3/2		-4.061800	-4.058148	1.964545	0.026325	Not Diff.
F4/2		-4.683240	-4.741563	1.964545	0.587787	Not Diff.
F5/2		-5.989467	-6.040235	1.964484	0.081374	Not Diff.
PFAVE	20.0	0.963476	0.963236	2.032245	0.712545	Not Diff.
DC60		-4.213128	-2.235046	2.015368	1.570975	Not Diff.
F1/2		-4.521381	-4.712421	1.964581	0.410748	Not Diff.
F2/2		-5.100615	-5.123860	1.964519	0.030367	Not Diff.
F3/2		-4.475898	-4.364658	1.964545	0.783785	Not Diff.
F4/2		-5.191977	-5.085143	1.964545	0.871927	Not Diff.
F5/2		-5.295521	-5.123356	1.964484	0.248050	Not Diff.

Table (26): Comparison of "Higher Order" and "Taguchi" Robust Design methodology, optimal Maximum HCF Life Expectancy mission.

Factor	α	LOG(Y_{LOR})	LOG(Y_{HOR})	t	t*	Comment
PFAVE	0.0	0.974070	0.973435	2.076075	1.313081	Not Diff.
DC60		-2.354837	-2.399085	2.054196	0.145369	Not Diff.
F1/2		-4.688334	-5.418904	1.967079	1.149451	Not Diff.
F2/2		-4.195049	-4.489256	1.966989	0.403095	Not Diff.
F3/2		-4.162474	-4.038721	1.967100	0.978353	Not Diff.
F4/2		-5.148175	-5.093419	1.967021	0.244374	Not Diff.
F5/2		-6.394333	-6.370093	1.966953	0.039097	Not Diff.
PFAVE	10.0	0.972330	0.971747	2.076075	1.447918	Not Diff.
DC60		-2.354837	-2.389396	2.053696	0.116031	Not Diff.
F1/2		-5.032574	-5.046314	1.967079	0.020808	Not Diff.
F2/2		-4.589592	-4.413385	1.966989	0.228640	Not Diff.
F3/2		-4.372424	-4.061800	1.967100	2.359925	Diff.
F4/2		-5.372825	-4.683240	1.967021	3.308468	Diff.
F5/2		-5.568553	-5.989467	1.966953	0.705987	Not Diff.
PFAVE	20.0	0.964227	0.963476	2.076075	1.553724	Not Diff.
DC60		-2.354837	-4.213128	2.054196	1.544704	Not Diff.
F1/2		-4.481273	-4.521381	1.967079	0.072862	Not Diff.
F2/2		-4.984091	-5.100615	1.966989	0.161440	Not Diff.
F3/2		-4.250998	-4.475898	1.967100	1.689247	Not Diff.
F4/2		-5.383004	-5.191977	1.967021	0.897072	Not Diff.
F5/2		-5.564421	-5.295521	1.966953	0.535833	Not Diff.

Table (27): Comparison of "Lower Order" and "Higher Order" Robust Design methodology, optimal Maximum HCF Life Expectancy mission.

REPORT DOCUMENTATION PAGE

Form Approved
OMB No. 0704-0188

Public reporting burden for this collection of information is estimated to average 1 hour per response, including the time for reviewing instructions, searching existing data sources, gathering and maintaining the data needed, and completing and reviewing the collection of information. Send comments regarding this burden estimate or any other aspect of this collection of information, including suggestions for reducing this burden, to Washington Headquarters Services, Directorate for Information Operations and Reports, 1215 Jefferson Davis Highway, Suite 1204, Arlington, VA 22202-4302, and to the Office of Management and Budget, Paperwork Reduction Project (0704-0188), Washington, DC 20503.

1. AGENCY USE ONLY (*Leave blank*)	2. REPORT DATE	3. REPORT TYPE AND DATES COVERED
	March 2002	Technical Memorandum

4. TITLE AND SUBTITLE

Robust Parameter Design Methodologies for Optimal Micro-Scale Secondary Flow Control in Compact Inlet Diffusers

5. FUNDING NUMBERS

WU–708–53–13–00

6. AUTHOR(S)

Bernhard H. Anderson and Dennis J. Keller

7. PERFORMING ORGANIZATION NAME(S) AND ADDRESS(ES)

National Aeronautics and Space Administration
John H. Glenn Research Center at Lewis Field
Cleveland, Ohio 44135–3191

8. PERFORMING ORGANIZATION REPORT NUMBER

E–13244

9. SPONSORING/MONITORING AGENCY NAME(S) AND ADDRESS(ES)

National Aeronautics and Space Administration
Washington, DC 20546–0001

10. SPONSORING/MONITORING AGENCY REPORT NUMBER

NASA TM—2002-211477

11. SUPPLEMENTARY NOTES

Bernhard H. Anderson, NASA Glenn Research Center, Cleveland, Ohio, and Dennis J. Keller, RealWorld Quality Systems, Cleveland, Ohio 44116. Responsible person, Bernhard H. Anderson, organization code 5850, 216–433–5822.

12a. DISTRIBUTION/AVAILABILITY STATEMENT

Unclassified - Unlimited
Subject Category: 07 Distribution: Nonstandard

Available electronically at http://gltrs.grc.nasa.gov/GLTRS
This publication is available from the NASA Center for AeroSpace Information, 301–621–0390.

12b. DISTRIBUTION CODE

13. ABSTRACT ***(Maximum 200 words)***

It is the purpose of this report to study and evaluate three optimal Robust design methodologies for application towards micro-scale secondary flow control (MSFC) for the management of inlet recovery, engine face distortion and High Cycle Fatigue (HCF) in compact inlet diffuser. The three Robust methodologies include (1) the traditional Taguchi *Robust Parameter Design* methodology, (2) a "Higher Order" Robust method, which used the same DOE structure as Taguchi, but with an alternate analysis, and (3) a "Lower Order" economical approach to Robust Design, where a single DOE was established which was composed of both the inner array (design) variables and outer array (mission) variables. Each of the three Robust methodologies examined in this report, (i.e., the Taguchi methodology, the "Higher Order" methodology, and the "Lower Order" methodology) provided installation designs that satisfied the mission requirements. Even though all three methodologies were capable of finding a robust optima that satisfied the mission requirements, the "Lower Order" method provides an economical alternative where the number of runs is drastically reduced.

14. SUBJECT TERMS	15. NUMBER OF PAGES
Aeronautics; Propulsion; Fluid dynamics	61
	16. PRICE CODE

17. SECURITY CLASSIFICATION OF REPORT	18. SECURITY CLASSIFICATION OF THIS PAGE	19. SECURITY CLASSIFICATION OF ABSTRACT	20. LIMITATION OF ABSTRACT
Unclassified	Unclassified	Unclassified	